

**METHODS FOR PILOT CONTAMINATION  
MITIGATION AND MAXIMIZATION OF SPECTRAL  
EFFICIENCY IN MASSIVE MIMO**

*A Project report submitted in partial fulfilment of the requirements for the award of  
the degree of*

**BACHELOR OF TECHNOLOGY IN  
ELECTRONICS AND COMMUNICATION ENGINEERING**

*Submitted by*

**S. Bhargav (318126512053)**

**S. Sai Nitish (318126512047)**

**Ankitha Hamsa (318126512002)**

**CH. Sri Harsha (318126512015)**

**Under the guidance of**

**Mr. B. Chandra Mouli**

**Asst.Professor-Department of ECE**



**DEPARTMENT OF ELECTRONICS AND COMMUNICATION  
ENGINEERING**

ANIL NEERUKONDA INSTITUTE OF TECHNOLOGY AND SCIENCES (UGC  
AUTONOMOUS) (*Permanently Affiliated to AU, Approved by AICTE and Accredited by NBA &  
NAAC with 'A' Grade*)Sangivalasa, Bheemilimandal, Visakhapatnam. (A.P) 2021-2022

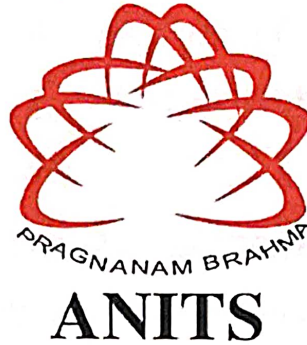
**DEPARTMENT OF ELECTRONICS AND COMMUNICATION**

**ENGINEERING**

**ANIL NEERUKONDA INSTITUTE OF TECHNOLOGY AND SCIENCES  
(UGC AUTONOMOUS)**

*(Permanently Affiliated to AU, Approved by AICTE and Accredited by NBA &  
NAAC with 'A' Grade)*

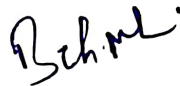
**Sangivalasa, Bheemili mandal, Visakhapatnam dist.(A.P)**



**CERTIFICATE**

*This is to certify that the project report entitled “Methods for Pilot Contamination Mitigation and Maximization of Spectral Efficiency in Massive MIMO” submitted by S. Bhargav (318126512053), Ankitha Hamsa (318126512002), CH. Sri Harsha (318126512015), Niteesh (318126512047) in partial fulfillment of the requirements for the award of the degree of Bachelor of Technology in Electronics & Communication Engineering of Andhra University, Visakhapatnam is a record of bonafide work carried out under my guidance and supervision.*

**Project Guide**



**Mr. B. Chandra Mouli**

**M. Tech, (Ph. D)**

**Department of E.C.E**

**ANITS**

**Assistant Professor  
Department of E.C.E.**

**Anil Neerukonda**

**Institute of Technology & Sciences  
Sangivalasa, Visakhapatnam-531 162**



**Head of the Department**

**Dr. V. Rajyalakshmi**

**Professor & HOD**

**Department of E.C.E**

**ANITS**

**Head of the Department  
Department of ECE**

**Anil Neerukonda Institute of Technology & Sciences  
Sangivalasa-531 162**

## **ACKNOWLEDGEMENT**

We would like to express our gratitude to our project guide **Mr.B.Chandra Mouli** , Department of Electronics and Communication Engineering, ANITS, for his guidance with unsurpassed knowledge and immense encouragement.

We are grateful to **Dr. V. Rajyalakshmi**, Head of the Department, Electronics and Communication Engineering, for providing us with the required facilities for the completion of the project work.

We are very much thankful to the **Principal and Management, ANITS, Sangivalasa**, for their encouragement and cooperation to carry out this work.

We express our thanks to all **teaching faculty** of Department of ECE, whose suggestions during reviews helped us in accomplishment of our project. We would like to thank **all non-teaching staff** of the Department of ECE, ANITS for providing great assistance in accomplishment of our project.

We would like to thank our parents, friends, and classmates for their encouragement throughout our project period. At last but not the least, we thank everyone for supporting us directly or indirectly in completing this project successfully.

### **PROJECT STUDENT**

**S. Bhargav (318126512053)**

**Ankitha Hamsa (318126512002)**

**CH. Sri Harsha (318126512015)**

**S. Sai Niteesh (318126512047)**

## ABSTRACT

Massive multiple-input multiple-output (MIMO) is widely acknowledged as the key enabling technology for the next-generation mobile communication networks. Pilot contamination (PC) is one of the key performance limiting factors for realizing the full potential offered by massive MIMO. It has an important impact beyond channel estimation, since the contamination makes it particularly hard for the BS to mitigate interference between UEs that use the same pilot. The mutual interference that these UEs cause during pilot transmission has two main consequences, the channel estimates become correlated and the estimation quality is reduced. So, in order to mitigate PC, optimal pilot allocation schemes are required. In our project, we have reviewed and compared two established methods that have provided a solution to mitigate the effect of pilot contamination. The two methods of interest are, one, a novel pilot decontamination scheme based on two existing schemes (soft pilot reuse and weighted-graphed-coloring based pilot decontamination) and two, a method based on large scale fading coefficients (The LSFC). Both the methods provide solutions with the help of the large-scale fading coefficients of the users. Since the user's large-scale fading coefficients depend on the distance between BSs and users, this characteristic parameter is exploited to classify users based on their LSF coefficients. Thereafter, pilots are assigned to users of different cells in both the methods. Both methods solve the problem of PC in their own way to optimally assign pilots. In the method one (SPR+WGC), all users are firstly separated into two categories based on their large-scale fading coefficients: cell centered users that reuse the same pilot sequences and cell edged users that use other orthogonal pilot subgroups to get rid of the severe contamination. But the slight contamination among the cell centered users still exists. Then, in order to improve the decontamination of cell centered users, a weighted-graph-based method is applied. The main disadvantage of this method is pilot overhead and in order to overcome this

drawback, we go for the second method based on LSF coefficients. In the method two (LSFC), the pattern where pilots are reused within different cells is considered. Specifically, the large-scale fading coefficients (LSFs) are exploited to show that the PC upon users depends on the distance between users that employ the same pilots. Hence, instead of optimizing the manner where pilots are assigned to users, the algorithm assigns pilots to users of different cells based on their LSF coefficients and through the exploitation of a simple matrix arrangement. The two methods are compared after thorough reviewing and simulation results show that the problem of PC is widely reduced with the LSFC method, while the SPR+WGC also significantly reduces PC.

## CONTENTS

<b>LIST OF FIGURES</b>	vii
<b>LIST OF TABLES</b>	viii
<b>LIST OF ABBREVIATIONS</b>	ix
<b>CHAPTER 1 INTRODUCTION</b>	
1.1 Project Objective	01
1.2 MIMO and earlier systems	02
<b>CHAPTER 2 INTRODUCTION TO MASSIVE MIMO</b>	
2.1 Introduction	05
2.2 Point to Point MIMO	05
2.3 Multiuser MIMO	07
2.4 Massive MIMO	09
2.5 Cellular Networks	12
2.6 Definition of Spectral Efficiency	14
2.7 Canonical Massive MIMO network	15
2.8 Small scale fading and large scale fading	17
2.9 Advantages Of Massive MIMO	18
2.10 Disadvantages Of Massive MIMO	20
<b>CHAPTER 3 PILOTS AND PILOT CONTAMINATION</b>	
3.1 Channel Estimation and the concept of Pilots	21
3.2 Acquiring Channel State Information	22
3.3 Coherence Time	23
3.4 Coherence Bandwidth	25
3.5 Coherence Interval	27
3.6 TDD Coherence Interval Structure	27

3.7	Coherence Blocks	28
3.8	Need for Pilots	30
3.9	Uplink Pilots and Channel Estimation	31
3.10	Orthogonal Pilots	31
3.11	Pilot Contamination	31
3.12	System Model for Uplink and Downlink	33
3.12.1	Uplink	33
3.12.1	Downlink	34
<b>CHAPTER 4 METHODS TO MITIGATE PILOT CONTAMINATION</b>		
4.1	Introduction to Pilot Contamination	36
4.2	Conventional Pilot Allocation Scheme	36
4.3	Approaches to Mitigate Pilot Contamination	38
4.3.1	Data-aided Channel Estimation	38
4.3.2	Pilot Assignment and Dimensioning	38
4.3.3	Multi-cell Cooperation	39
4.4	Methods to Mitigate Pilot Contamination	40
4.4.1	Methods taken into Consideration	40
4.4.2	Soft Pilot Reuse Scheme and Weighted Graph Coloring Method	40
4.4.3	Strategy based on Large Scale Fading Coefficients	49
4.5	Comparison Table	55
<b>CHAPTER 5 RESULTS AND DISCUSSIONS</b>		
5.1	Simulation Results	57
<b>CONCLUSIONS</b>		62
<b>REFERENCES</b>		65

## LIST OF FIGURES

<b>Figure no</b>	<b>Title</b>	<b>Page no</b>
Fig 1.1	SISO	02
Fig 1.2	SIMO	03
Fig 1.3	MISO	04
Fig 1.4	MIMO	04
Fig 2.1	Point to Point MIMO	07
Fig 2.2	Multi User MIMO	07
Fig 2.3	Massive MIMO	10
Fig 2.4	Cellular Network in Massive MIMO	13
Fig 3.1	Obtaining accurate CSI in multiuser MIMO	21
Fig 3.2	Antenna at the BS receiving pilot signal	23
Fig 3.3	Two Path Propagation model	24
Fig 3.4	Coherence Time and Coherence Bandwidth	25
Fig 3.5	Allocation of the samples in a coherence interval	28
Fig 3.6	Coherence Block	29
Fig 3.7	UL Pilot, UL Data, DL Data, Sub-Carrier	29
Fig 3.8	Pilot Contamination Illustration	32
Fig 3.9	Illustration of Uplink Transmission	34
Fig 4.1	Examples of Pilot reuse factors	37
Fig 4.2	Soft Pilot Reuse Scheme	43
Fig 4.3	User Division in SPRS	44
Fig 4.4	Potential ICI	45
Fig 4.5	WGC+SPRS Scheme Illustration	46
Fig 4.6	User Classification Based on LSF Coefficient	51
Fig 4.7	LSFC Strategy	52
Fig 4.8	Matrix Arrangement	53
Fig 4.9	Pilot Assignment Based on P Matrix	53
Fig 5.1	CDF vs SINR	58
Fig 5.2	CDF vs R	59
Fig 5.3	R vs M	60
Fig 5.4	R vs Transmission Power	61



## LIST OF TABLES

<b>Table No</b>	<b>Title</b>	<b>Page No</b>
Table 4.1	Comparison of the Two Methods of Interest	55
Table 5.1	Parameters in Simulation	57

## **LIST OF ABBREVIATIONS**

SISO	Single Input Single Output
SIMO	Single Input Multiple Output
MISO	Multiple Input Single Output
MIMO	Multiple Input Multiple Output
M-MIMO	Massive- Multiple Input Multiple Output
FDD	Frequency Division Duplexing
TDD	Time Division Duplexing
RF	Radio Frequency
CSI	Channel State Information
JSDM	Joint Spatial Division Multiplexing
SPRS	Soft Pilot Reuse Scheme
LSFC	Large Scale Fading Coefficients
WGC-PD	Weighted Graph Coloring-Pilot Decontamination
AWGN	Additive White Gaussian Noise
WGC-SPR	Weighted Graph Coloring- Soft Pilot Reuse
LSF	Large Scale Fading
SSF	Small Scale Fading

# CHAPTER 1

## INTRODUCTION

### 1.1 Project Objective:

Massive MIMO communication architecture has recently emerged as a new paradigm for wireless communications in the multi-path environment. These antenna systems potentially allow base stations (BSs) to operate with huge improvements in spectral and radiated energy efficiency, using relatively low-complexity linear processing. The higher spectral efficiency is attained by serving several terminals in the same time-frequency resource through spatial multiplexing, and the increase in energy efficiency is mostly due to the array gain provided by the large set of antennas. The expected massive MIMO improvements assume that accurate channel estimations are available at both the receiver and transmitter for detection and precoding, respectively. Additionally, the reuse of frequencies and pilot reference sequences in cellular communication systems causes interferences in channel estimation, degrading its performance. Since both the time-frequency resources allocated for pilot transmission and the channel coherence time are limited, the number of possible orthogonal pilot sequences is also limited, and as a consequence, the pilot sequences have to be reused in neighbor cells of cellular systems. Therefore, channel estimates obtained in a given cell get contaminated by the pilots transmitted by the users in other cells. This coherent interference is known in the literature as pilot contamination, i.e., the channel estimate at the base station in one cell becomes contaminated by the pilots of the users from other cells. The contamination not only reduces the quality of the channel estimates, i.e., increases the MSE, but also makes the channel estimates statistically dependent, even though the true channels are statistically independent. Moreover, pilot contamination does not disappear with the addition of more antennas. In a real-world network deployment, although changing slowly, the large-scale fading coefficients must be estimated and updated from time to time. Additionally, the estimation error of the large-scale fading coefficients impacts

significantly on the performance of uplink data decoding and downlink transmission (e.g., precoding and beamforming).

In this work, we examined the methods to mitigate pilot contamination in massive MIMO. Consequently, we compare two methods that have been previously proposed and simulation results are produced to find insights.

## 1.2 MIMO and Earlier Systems:

### 1.2.1 SISO:

In control engineering, a single-input and single-output (*SISO*) *system* is a simple single variable control system with one input and one output. In radio it is the use of only one antenna both in the transmitter and receiver. SISO is the simplest antenna technology. In some environments, SISO systems are vulnerable to problems caused by multipath effects. When an electromagnetic field (EM field) is met with obstructions such as hills, canyons, buildings, and utility wires, the wavefronts are scattered, and thus they take many paths to reach the destination. The late arrival of scattered portions of the signal causes problems such as fading, cut-out (cliff effect), and intermittent reception (picket fencing). In a digital communications system, it can cause a reduction in data speed and an increase in the number of errors.



Figure 1.1:- SISO -Single Input Single Output

### 1.2.2 SIMO

The SIMO or Single Input Multiple Output version of MIMO occurs where the transmitter has a single antenna and the receiver has multiple antennas. This

is also known as receive diversity. It is often used to enable a receiver system that receives signals from a number of independent sources to combat the effects of fading. It has been used for many years with short wave listening / receiving stations to combat the effects of ionospheric fading and interference.

SIMO has the advantage that it is relatively easy to implement although it does have some disadvantages in that the processing is required in the receiver. The use of SIMO may be quite acceptable in many applications, but where the receiver is located in a mobile device such as a cellphone handset, the levels of processing may be limited by size, cost and battery drain.

There are two forms of SIMO that can be used:

- **Switched diversity SIMO:** This form of SIMO looks for the strongest signal and switches to that antenna.
- **Maximum ratio combining SIMO:** This form of SIMO takes both signals and sums them to give the combination. In this way, the signals from both antennas contribute to the overall signal.



**Figure 1.2:-** SIMO Single Input Multiple Output

### 1.2.3 MISO

MISO is also termed transmit diversity. In this case, the same data is transmitted redundantly from the two transmitter antennas. The receiver is then able to receive the optimum signal which it can then use to receive extract the required data.



**Figure 1.3:-** MISO Multiple Input Single Output

The advantage of using MISO is that the multiple antennas and the redundancy coding / processing is moved from the receiver to the transmitter. In instances such as cellphone UEs, this can be a significant advantage in terms of space for the antennas and reducing the level of processing required in the receiver for the redundancy coding.

#### 1.2.4 MIMO

Control Systems, where there is more than one antenna at either end of the radio link, this is termed MIMO - Multiple Input Multiple Output. MIMO can be used to provide improvements in both channel robustness as well as channel throughput.



**Figure 1.4:-** MIMO- Multiple Input Multiple Output

In order to be able to benefit from MIMO fully it is necessary to be able to utilize coding on the channels to separate the data from the different paths. This requires processing, but provides additional channel robustness / data throughput capacity. There are many formats of MIMO that can be used from SISO, through SIMO and MISO to the full MIMO systems. These are all able to provide significant improvements of performance, but generally at the cost of additional processing and the number of antennas used. Balances of performance against costs, size, processing available and the resulting battery life need to be made when choosing the correct option.

## CHAPTER 2

### INTRODUCTION TO MASSIVE MIMO

#### 2.1 Introduction:

The performance limitation of any wireless network will always be at the physical layer, because, fundamentally, the amount of information that can be transferred between two locations is limited by the availability of spectrum, the laws of electromagnetic propagation, and the principles of information theory. There are three basic ways in which the efficiency of a wireless network may be improved: (i) deploying access points more densely; (ii) using more spectrum; and (iii) increasing the spectral efficiency, that is, the number of bits that can be conveyed per second in each unit of bandwidth. While future wireless systems and standards are likely to use an ever-increasing access point density and use new spectral bands, the need for maximizing the spectral efficiency in a given band is never going to vanish. The use of multiple antennas, also known as multiple-input, multiple-output (MIMO) technology, is the only viable approach for substantial improvement of spectral efficiency. While mostly developed during the last two decades, it is noteworthy that a basic idea behind MIMO is almost a century old directional beamforming using an antenna array was suggested to permit more aggressive frequency reuse of scarce spectrum – in this case, very low frequency – for transoceanic communication. MIMO technology is logically classified into one of three categories, whose development occurred during roughly disjoint epochs: Point-to-Point MIMO, Multiuser MIMO, and Massive MIMO.

#### 2.2 Point-to-Point MIMO

Point-to-Point MIMO emerged in the late 1990s and represents the simplest form of MIMO: a base station equipped with an antenna array serves a terminal equipped with an antenna array; see Figure 2.1. Different terminals are orthogonally multiplexed, for example via a combination of time- and frequency-division multiplexing. In what follows, we summarize some basic facts about Point-to-Point MIMO. More details, along with derivations of all formulas given here. In each channel

use, a vector is transmitted and a vector is received. In the presence of additive white Gaussian noise at the receiver, Shannon theory yields the following formulas for the link spectral efficiency (in b/s/Hz):

$$C_{ul} = \log_2 | \mathbf{M} + \rho_{ul} \mathbf{K} \mathbf{G} \mathbf{G}^H | \quad C_{nl} = \log_2 \quad (2.1)$$

$$C_{dl} = \log_2 | \mathbf{K} + \rho_{dl} \mathbf{M} \mathbf{G} \mathbf{G}^H | \quad (a) = \log_2 | \mathbf{M} + \rho_{dl} \mathbf{M} \mathbf{G} \mathbf{G}^H | \quad (2.2)$$

In (1.1) and (1.2),  $\mathbf{G}$  is an  $M \times K$  matrix that represents the frequency response of the channel between the base station array and the terminal array;  $\rho_{ul}$  and  $\rho_{dl}$  are the uplink and downlink signal-to-noise ratios (SNRs), which are proportional to the corresponding total radiated powers;  $M$  is the number of base station antennas; and  $K$  is the number of terminal antennas. The normalization by  $K$  and  $M$  reflects the fact that for constant values of  $\rho_{ul}$  and  $\rho_{dl}$  total radiated power is independent of the number of antennas. The spectral efficiency values in (1.1) and (1.2) require the receiver to know  $\mathbf{G}$  but do not require the transmitter to know  $\mathbf{G}$ . Performance can be improved somewhat if the transmitter also acquires channel state information (CSI). However, this requires special effort and is seldom seen in practice. In isotropic (rich) scattering propagation environments, well modeled by independent Rayleigh fading, for sufficiently high SNRs,  $C_{ul}$  and  $C_{dl}$  scale linearly with  $\min(M, K)$  and logarithmically with the SNR. Hence, in theory, the link spectral efficiency can be increased by simultaneously using large arrays at the transmitter and the receiver, that is, making  $M$  and  $K$  large. In practice, however, three factors seriously limit the usefulness of Point-to-Point MIMO, even with large arrays at both ends of the link. First, the terminal equipment is complicated, requiring independent RF chains per antenna as well as the use of advanced digital processing to separate the data streams. Second, more fundamentally, the propagation environment must support  $\min(M, K)$  independent streams. This is often not the case in practice when compact arrays are used. Line-of-sight (LoS) conditions are particularly stressing. Third, near the cell edge, where normally a majority of the terminals are located and where SNR is typically low because of high path loss, the spectral efficiency scales slowly with  $\min(M, K)$ .



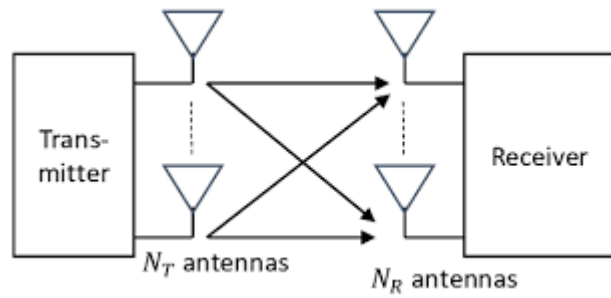


**Figure 2.1:-** Point-to-Point MIMO.

### 2.3 Multiuser MIMO

The idea of Multiuser MIMO is for a single base station to serve a multiplicity of terminals using the same time-frequency resources; see Figure 2.2. Effectively, the Multiuser MIMO scenario is obtained from the Point-to-Point MIMO setup by breaking up the K-antenna terminal into multiple autonomous terminals. The basic concept of serving several terminals simultaneously using an antenna array at the base station is quite old.

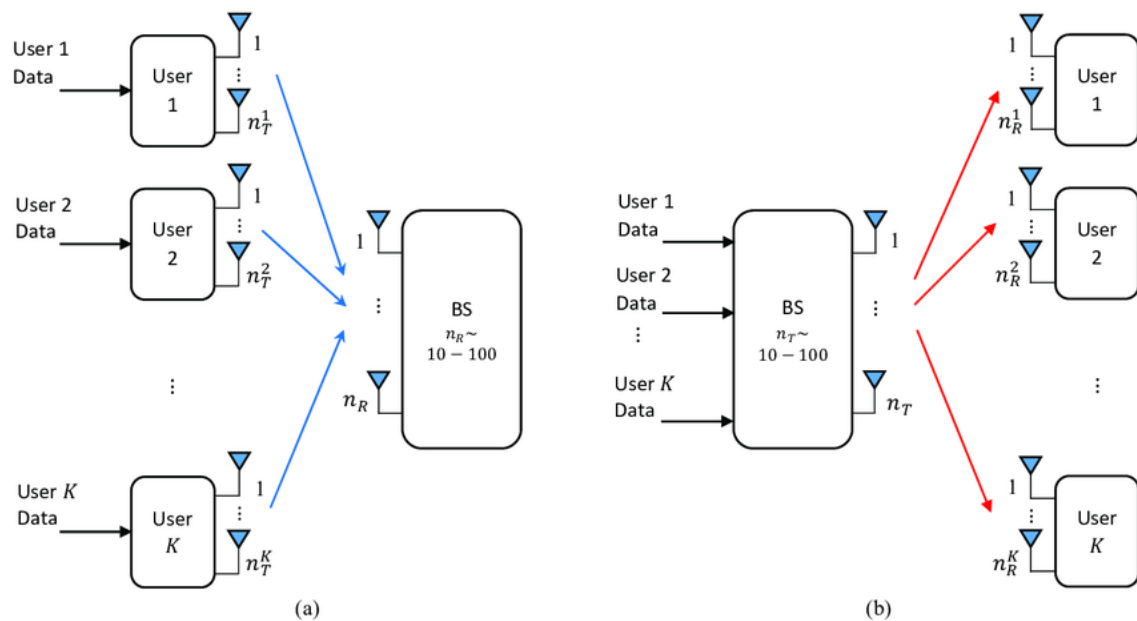


**Fig 2.2:-** Multiuser MIMO

The uplink and downlink sum spectral efficiencies are given by:

$$C_{ul} = \log_2 \left( I + \rho_{ul} \mathbf{G} \mathbf{G}^H \right) \quad (2.3)$$

$$C_{dl} = \max_{\mathbf{v} \geq \mathbf{0}} \sum_{k=1}^K v_k \log_2 \left( I + \rho_{dl} \mathbf{G} \mathbf{D} \mathbf{v} \mathbf{G}^H \right) \quad (2.4)$$

where  $\mathbf{v} = [v_1, \dots, v_K]^T$ ,  $\rho_{ul}$  is the uplink SNR per terminal, and  $\rho_{dl}$  is the downlink SNR. (For given  $\rho_{ul}$ , the total uplink power is  $K$  times greater than for the Point-to-Point MIMO. The computation of downlink capacity according to (1.4) requires the solution of a convex optimization problem. The possession of CSI is crucial to both (1.3) and (1.4). On uplink, the base station alone must know the channels, and each terminal has to be told its permissible transmission rate separately. On the downlink, both the base station and the terminals must have CSI. Note that the terminal antennas in the point-to-point case can cooperate, whereas the terminals in the multiuser case cannot. Quite remarkably, however, the inability of the terminals to cooperate in the multiuser system does not compromise the uplink sum spectral efficiency as seen by comparing (1.1) and (1.3). Note also that the downlink capacity (1.4) may exceed the downlink capacity in (1.2) for Point-to-Point MIMO, because (1.4) assumes that the base station knows  $\mathbf{G}$ , whereas (1.2) does not. Multiuser MIMO has two fundamental advantages over Point-to-Point MIMO. First, it is much less sensitive to assumptions about the propagation environment. For example, LoS conditions are stressing for Point-to-Point MIMO, but not for Multiuser MIMO, as explained in Chapter 7. Second, Multiuser MIMO requires only single-antenna terminals. Notwithstanding these virtues, two factors seriously limit the practicality of Multiuser MIMO in its originally conceived form. First, to achieve the spectral efficiencies in (1.3) and (1.4) requires complicated signal processing by both the base station and the terminals. Second, and more seriously, on the downlink both the base station and the terminals must know  $\mathbf{G}$ , which requires substantial resources to be set aside for transmission of pilots in both directions. For these reasons, the original form of Multiuser MIMO is not scalable either with respect to  $M$  or to  $K$ .

## 2.4 Massive MIMO

Massive MIMO is a useful and scalable version of Multiuser MIMO. This section introduces the basic Massive MIMO concepts. Consideration of net spectral efficiency alone according to the rigorous Shannon theory that underlies (1.3) and (1.4) suggests the optimality of a rough parity between  $M$  and  $K$  in conventional Multiuser MIMO: further growth of  $M$  only yields logarithmically increasing throughputs while incurring linearly increasing amounts of time spent on training. Massive MIMO represents a clean break from conventional Multiuser MIMO. Measures are taken such that one operates farther from the Shannon limit, but paradoxically achieves much better performance than any conventional Multiuser MIMO system. There are three fundamental distinctions between Massive MIMO and conventional Multiuser MIMO. First, only the base station learns  $G$ . Second,  $M$  is typically much larger than  $K$ , although this does not have to be the case. Third, simple linear signal processing is used both on the uplink and on the downlink. These features render Massive MIMO scalable with respect to the number of base station antennas.

Each base station is equipped with a large number of antennas,  $M$ , and serves a cell with a large number of terminals,  $K$ . The terminals typically (and throughout this book) have a single antenna each. Different base stations serve different cells, and with the possible exception of power control and pilot assignment, Massive MIMO uses no cooperation among base stations. Either in uplink or in downlink transmissions, all terminals occupy the full time-frequency resources concurrently. On uplink, the base station has to recover the individual signals transmitted by the terminals. On the downlink, the base station has to ensure that each terminal receives only the signal intended for it. The base station's multiplexing and de-multiplexing signal processing is made possible by utilizing a large number of antennas and by its possession of CSI. Under LoS propagation conditions, the base station creates, for each terminal, a beam within a narrow angular window centered around the direction to the terminal. The more antennas, the narrower are the beams. By contrast, in the presence of local scattering, the signal seen at any given point in space is the superposition of many independently scattered and reflected components that may add up constructively

or destructively. When the transmitted waveforms are properly chosen, these components superimpose constructively precisely at the locations of the terminals.

The more antennas, the more sharply the power focuses onto the terminals. When focusing the power, the use of sufficiently accurate CSI at the base station is essential. In time-division duplex operation (TDD), the base station acquires CSI by measuring pilots transmitted by the terminals, and exploiting reciprocity between the uplink and downlink channel. This requires reciprocity calibration of the transceiver hardware. However, phase-calibrated arrays are not required, since by virtue of the reciprocity a phase offset between any two antennas will affect the uplink and the downlink in the same way. Increasing the number of antennas,  $M$ , always improves performance, in terms of both reduced radiated power and in terms of the number of terminals that can be simultaneously served. Larger than  $K$ , although this does not have to be the case. Third, simple linear signal processing is used both on the uplink and on the downlink. These features render Massive MIMO scalable with respect to the number of base station antennas,  $M$ . Figure 2.3 illustrates the basic Massive MIMO setup. Each base station is equipped with a large number of antennas,  $M$ , and serves a cell with a large number of terminals,  $K$ . The terminals typically (and throughout this book) have a single antenna each.



**Figure 2.3:-** Massive MIMO

Different base stations serve different cells, and with the possible exception of power control and pilot assignment, Massive MIMO uses no cooperation among base stations. Either in uplink or in downlink transmissions, all terminals occupy the full time-frequency resources concurrently. On uplink, the base station has to recover the individual signals transmitted by the terminals. On the downlink, the base station has to ensure that each terminal receives only the signal intended for it. The base station's multiplexing and de-multiplexing signal processing is made possible by utilizing a large number of antennas and by its possession of CSI.

Under LoS propagation conditions, the base station creates, for each terminal, a beam within a narrow angular window centered around the direction to the terminal. The more antennas, the narrower are the beams. By contrast, in the presence of local scattering, the signal seen at any given point in space is the superposition of many independently scattered and reflected components that may add up constructively or destructively. When the transmitted waveforms are properly chosen, these components superimpose constructively precisely at the locations of the terminals. The more antennas, the more sharply the power focuses onto the terminals. When focusing the power, the use of sufficiently accurate CSI at the base station is essential. In time-division duplex operation (TDD), the base station acquires CSI by measuring pilots transmitted by the terminals, and exploiting reciprocity between the uplink and downlink channel. This requires reciprocity calibration of the transceiver hardware. However, phase-calibrated arrays are not required, since by virtue of the reciprocity a phase offset between any two antennas will affect the uplink and the downlink in the same way. Increasing the number of antennas,  $M$ , always improves performance, in terms of both reduced radiated power and in terms of the number of terminals that can be simultaneously served. The use of large numbers of antennas at the base station is instrumental not only to obtain high sum spectral efficiencies in a cell, but, more importantly, to provide uniformly good service to many terminals simultaneously. An additional consequence of using large numbers of antennas is that the required signal processing and resource allocation simplifies, owing to a phenomenon known as channel hardening. The significance of channel hardening is that effects of small-scale fading and frequency dependence disappear when  $M$  is large.

Specifically, consider a terminal with  $M$ -dimensional channel response  $g$ ; if beamforming with a beamforming vector  $a$  is applied, then the terminal sees a scalar channel with gain  $aTg$ . When  $M$  is large, by virtue of the law of large numbers,  $aTg$  is close to its expected value,  $E aTg$  (a deterministic number). This means that the resulting effective channel between each terminal and the base station is a scalar channel with known, frequency-independent gain and additive noise. Importantly, this characterization does not rely on channel hardening and it is valid for any  $M$  and  $K$ ;

however, by virtue of channel hardening, most relevant capacity bounds are tight only when  $M$  is reasonably large.

This characterization in turn facilitates the use of simple schemes for resource allocation and power control. Furthermore, channel hardening renders channel estimation at the terminals, and the associated transmission of downlink pilots, unnecessary in most cases. Another benefit of channel hardening in Massive MIMO is that the effective scalar channel seen by each terminal behaves much like an additive white Gaussian noise (AWGN) channel, and hence standard coding and modulation techniques devised for the AWGN channel tend to work well.

## **2.5 Cellular Networks**

Wireless communication is based on radio, meaning that electromagnetic(EM) waves are designed to carry information from a transmitter to one or multiple receivers. Since the EM waves propagate in all possible directions from the transmitter, the signal energy spreads out and less energy reaches a desired receiver as the distance increases. To deliver wireless services with sufficiently high received signal energy over wide coverage areas, researchers at Bell Labs postulated in 1947 that a cellular network topology is needed. According to this idea, the coverage area is divided into cells that operate individually using a fixed-location base station; that is, a piece of network equipment that facilitates wireless communication between a device and the network. The cellular concept was further developed and analyzed over the subsequent decades and later deployed in practice. Without any doubt, the cellular concept was a major breakthrough and has been the main driver to deliver wireless services in the last forty years (since the “first generation” of mobile phone systems emerged in the 1980s). In this monograph, a cellular network is defined as follows.

### **2.5.1 Cellular network**

A cellular network consists of a set of base stations (BSs) and a set of user equipment (UEs). Each UE is connected to one of the BSs, which provides

service to it. The downlink (DL) refers to signals sent from the BSs to their respective UEs, while the uplink (UL) refers to transmissions from the UEs to their respective BSs. While this definition specifies the setup that we will study, it does not cover every aspect of cellular networks; for example, to enable efficient handover between cells, a UE can momentarily be connected to multiple BSs. There are several branches of wireless technologies that are currently in use, such as the IEEE 802.11 family for Wi-Fi wireless local area networks (WLANs), the 3rd Generation Partnership Project (3GPP) family with GSM/UMTS/LTE for mobile communications and the competing 3GPP2 family with IS-95/CDMA2000/EV-DO. Some standards within these families are evolutions of each other, optimized for the same use case, while others are designed for different use cases. Together they form a heterogeneous network consisting of two main tiers:

1. Coverage tier: Consisting of outdoor cellular BSs that provide wide-area coverage, mobility support, and are shared between many UEs.
2. Hotspot tier: Consisting of (mainly) indoor BSs that offer high throughput in small local areas to a few UEs. The term “heterogeneous” implies that these two tiers coexist in the same area. BS in coverage tier BS in hotspot tier UE in any tier.

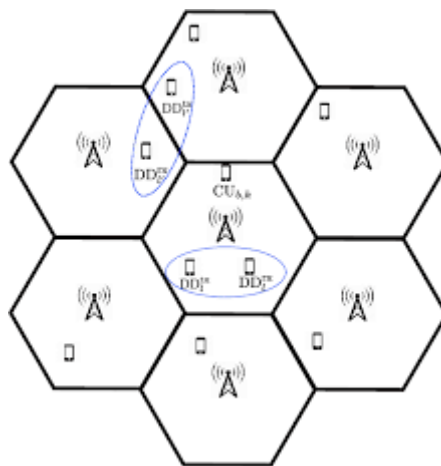


**Figure 2.4:- Cellular Network in Massive MIMO**

The two tiers may utilize the same frequency spectrum, but, in practice, it is common to use different spectrum to avoid inter-tier coordination; for example, the coverage tier might use LTE and operate in the 2.1 GHz band, while the hotspot tier

might use WIFI in the 5 GHz band. Cellular networks were originally designed for wireless voice communications, but it is wireless data transmissions that dominate nowadays [109]. Video on-demand accounts for the majority of traffic in wireless networks and is also the main driver of the predicted increase in traffic demand. The area throughput is thus a highly relevant performance metric of contemporary and future cellular networks. It is measured in bit/s/km<sup>2</sup> and can be modeled using the following high-level formula:

$$\text{Area throughput} = [\text{bit/s/km}^2] = B [\text{Hz}] \cdot D [\text{cells/km}^2] \cdot \text{SE} [\text{bit/s/Hz/cell}] \quad (2.5)$$

where B is the bandwidth, D is the average cell density, and SE is the SE per cell. The SE is the amount of information that can be transferred per second over one Hz of bandwidth. These are the three main components that determine the area throughput, and that need to be increased in order to achieve higher area throughput in future cellular networks. This principle applies to the coverage tier as well as to the hotspot tier. Based on (1.5), one can think of the area throughput as being the volume of a rectangular box with sides B, D, and SE. There is an inherent dependence between these three components in the sense that the choice of frequency band and cell density affects the propagation conditions; for example, the probability of having a line-of-sight (LoS) channel between the transmitter and receiver (and between out-of-cell interferers and the receiver), the average propagation losses, etc. However, one can treat these three components as independent as a first-order approximation to gain basic insights. Consequently, there are three main ways to improve the area throughput of cellular networks:

1. Allocate more bandwidth;
2. Densify the network by deploying more BSs;
3. Improve the SE per cell.

## 2.6 Definition of Spectral Efficiency

The SE of an encoding/decoding scheme is the average number of bits of information, per complex-valued sample, that it can reliably transmit over the channel under consideration. From this definition, it is clear that the SE is a



deterministic number that can be measured in bit per complex-valued sample. Since there are  $B$  samples per second, an equivalent unit of the SE is bit per second per Hertz, often written in short-form as bit/s/Hz. For fading channels, which change over time, the SE can be viewed as the average number of bit/s/Hz over the fading realizations, as will be defined below. In this monograph, we often consider the SE of a channel between a UE and a BS, which for simplicity we refer to as the “SE of the UE”. A related metric is the information rate [bit/s], which is defined as the product of the SE and the bandwidth  $B$ . In addition, we commonly consider the sum SE of the channels from all UEs in a cell to the respective Base Station, which is measured in bit/s/Hz/cell. The channel between a transmitter and a receiver at given locations can support many different SEs (depending on the chosen encoding/decoding scheme), but the largest achievable SE is of key importance when designing communication systems. The maximum SE is determined by the channel capacity, which was defined by Claude Shannon in his seminal paper from 1948.

## **2.7(Canonical Massive MIMO network)**

A Massive MIMO network is a multicarrier cellular network with  $L$  cells that operate according to a synchronous TDD protocol.<sup>1</sup> BS  $j$  is equipped with  $M_j > 1$  antennas, to achieve channel hardening. BS  $j$  communicates with  $K_j$  single-antenna UEs simultaneously on each time/frequency sample, with antenna-UE ratio  $M_j/K_j > 1$ . Each BS operates individually and processes its signals using linear receive combining and linear transmit precoding.

We consider this as the canonical form of Massive MIMO because it has the characteristics listed above and is in line with Marzetta’s seminal work. It also represents the technology that has been demonstrated in real-time Massive MIMO testbeds. However, there are important research efforts that deviate from the canonical form (or attempt to broaden it). In particular, finding an efficient FDD protocol for Massive MIMO is highly desirable, since there are vast amounts of spectrum reserved for FDD operation. In mobile scenarios, the estimation/feedback overhead of FDD operation is prohibitive, unless something is done to reduce it. The predominant

approach is to parameterize the channel and utilize the parametrization to reduce the channel estimation and feedback overhead. These works are based on the hypothesis that the channels can be parameterized in a particular way, which is then utilized to achieve a more efficient estimation and feedback procedure. However, this line of research is still in its infancy since the underlying hypothesis has not been proved experimentally. This is why FDD operation is not considered in this monograph, but we stress that designing and demonstrating an efficient FDD Massive MIMO implementation is a great challenge that needs to be tackled .

Two other deviations from the canonical form of Massive MIMO are the use of multiantenna UEs and single-carrier transmission. The propagation channels change over time and frequency. The bandwidth  $B$  equals the number of complex-valued samples that describe the signal per second. The time interval between two samples thus decreases as the bandwidth increases. Wireless channels are dispersive, meaning that the signal energy that is transmitted over a given time interval spreads out and is received over a longer time interval. If the sample interval is short, as compared to the dispersiveness of the channel, there will be a substantial overlap between adjacent transmitted samples at the receiver. The channel then has memory, which makes it harder to estimate it and to process the transmitted and received signal to combat inter-sample interference. A classic solution is to divide the bandwidth into many subcarriers, each having a sufficiently narrow bandwidth so that the effective time interval between samples is much longer than the channel dispersion.

The important thing from the Massive MIMO perspective is not which multicarrier modulation scheme is used, but that the frequency re-sources are divided into flat-fading subcarriers. The coherence bandwidth  $B_c$  describes the frequency interval over which the channel responses are approximately constant. One or multiple subcarriers fit(s) into the coherence bandwidth, thus the channel observed on adjacent subcarriers are either approximately equal or closely related through a deterministic transformation. Hence, there is generally no need to estimate the channel on every subcarrier. Similarly, the time variations of the channels are small between adjacent samples and the

coherence time  $T_c$  describes the time interval over which the channel responses are approximately constant.

## 2.8 Small-Scale and Large-Scale Fading

*Large scale-fading* represents the average signal-power attenuation or path loss due to motion over large areas and it is impacted by terrain configuration between the transmitter and receiver, and over a very long distance (several hundreds or thousands of meters), there is a steady decrease in power. Examination of the power over such a distance reveals that the power fluctuates around a mean value and these fluctuations have a rather long period. The statistics of large-scale fading, described in terms of a mean-path loss ( $n^{\text{th}}$ -power law) and a log-normally distributed variation about the mean, can lead to an estimate of path loss as a function of distance.

*Small-scale fading* refers to the rapid changes of the amplitude and phase of a radio signal over a short period of time (on the order of seconds) or a short distance (a few wavelengths). In small-scale fading, the instantaneous received signal power may vary as much as 30 to 40 dB when the receiver is moved by only a fraction of a wavelength. In a mobile-radio environment, each path has its own Doppler shift, time delay, and path attenuation, and multipath propagation results in a time-varying signal as the mobile moves position. Such a channel is linear, but time-varying. Small-scale fading is also called Rayleigh fading because when the number of versions of the transmitted signal which arrive at slightly different times is large, the envelope of the received signal is statistically described by a Rayleigh distribution if there is no line-of-sight component. If there is a line-of-sight component, it is then described by a Rician distribution. Small-scale fading depends on the nature of the transmitted signal with respect to the characteristics of the channel. Depending on the relation between the signal parameters, such as the bandwidth and the symbol period, on the one hand, and the channel parameters, such as the coherence time, Doppler spread, coherence bandwidth and delay spread, on the other hand, different transmitted signals will experience different types of fading. Delay spread leads to time dispersion and frequency-selective fading. Doppler spread leads to frequency dispersion and time-selective fading. Time dispersion and frequency dispersion are caused by independent

propagation mechanisms. Within a coherence interval, the complex-valued gain between any pair of antennas is substantially constant, and is denoted by the symbol  $g$ . It is useful to factor  $g$  as follows:

$$g = \beta h \quad (2.6)$$

The positive real number,  $\beta$ , called the large-scale fading coefficient, embodies range dependent path loss and shadow fading, it is virtually independent of frequency, and is strongly correlated over many wavelengths of space. The complex-valued number  $h$ , representing small-scale fading, models range dependent phase shift and constructive and destructive interference among different propagation paths. In all ensuing analyses, we will assume that the small-scale fading is Rayleigh; that is,  $h \sim \text{CN}(0, 1)$ . The assumption of Rayleigh fading permits the use of Bayesian analysis and it makes ergodic capacity a legitimate performance criterion. Rayleigh fading is also straightforward to justify with simple physical models. For example, in isotropic scattering,  $h$  represents the combined effect of many independent propagation paths so by the superposition principle and the central limit theorem,  $h$  will be approximately circularly symmetric Gaussian.

## 2.9 Advantages Of Massive MIMO

Following are the Advantages of Massive MIMO (M-MIMO) system:

### 1. Increases Network Capacity

Massive MIMO increases the capacity of a particular wireless communication network in two ways. First, it enables the deployment of higher frequencies. Second, by employing multi-user MIMO, a cellular base station with Massive MIMO capability can send and receive multiple data streams simultaneously from different users using the same frequency resources.

Note that network capacity is determined by the number or amount of total data a particular network can serve to its end-users, as well as by the maximum number of end-users that can be served based on an expected service level.

## **2. Enhances Network Coverage**

Another advantage of Massive MIMO is that it provides high spectral efficiency through the coordination of multiple antennas using simple processing and without intensive power consumption. When used in a 5G cellular network technology, it allows 10 times more spectral and network efficiency compared to fourth-generation networks. Furthermore, when applied in 4G technology, it improves the deep coverage of fourth-generation networks.

Because next-generation cellular network technologies use electromagnetic radiation with higher frequencies or more specifically, frequencies within the upper limits of radio waves and the range of microwaves, the signals they generate travel a short distance. Hence, enhancing network coverage is critical in modern and future cellular technologies.

## **3. Complements Beamforming**

Beamforming technology works by focusing a signal toward a specific direction, rather than broadcasting in all directions, thus resulting in more direct communication between a transmitter and a receiver, more stable and reliable connectivity, and faster data transmission. As a signal processing technique and traffic-signaling system, this technology depends on advanced antenna technologies on both access points and end-user devices.

The large number of antennas in a Massive MIMO system enables three-dimensional beamforming in which a single beam of signal-bearing electromagnetic radiation travels through vertical and horizontal directions. The process increases data transmission rates further while reaching people in elevated areas such as buildings and those in moving vehicles

## **4. Enables Next-Gen Technologies**

Massive MIMO is an essential component of 5G technology. For example, in Sub-6 5G specification, it allows the utilization of frequencies within the sub-6 GHz range. Moreover, in mmWave 5G specification, this technology increases frequency reach to expand network coverage, optimizes the propagation of signal-bearing electromagnetic radiation, and allows true multi-user wireless communication within a defined area.

However, although it is a key enabling technology for 5G and future cellular network technologies, it has been used for improving and repurposing the capabilities of existing 4G systems, especially LTE Advanced networks. The integration of Massive MIMO in existing 4G networks could improve further network performance.

## 2.10 DISADVANTAGES OF MASSIVE MIMO TECHNOLOGY

One of the biggest disadvantages of Massive MIMO is the cost associated with its implementation and deployment. The systems are several times more extensive than traditional base station units and antenna technologies.

Furthermore, the design of multiple antenna systems for cellular networks is more complex and requires more effort and time during assembly and installation.

Following are the drawbacks or **disadvantages of Massive MIMO**:

- ➔ Massive MIMO units are several times expensive compare to traditional radio units.
- ➔ Massive MIMO antenna designs are more complex and requires more effort and time during assembly line compare to traditional antenna designs.
- ➔ Use of FDD in massive MIMO leads to feedback overhead. This overhead increases with increase in antenna elements. Hence TDD is used due to its channel reciprocity concept.
- ➔ Spacing between antennas is very less and hence requires packing of entire hardware into smaller space. For example, 32T32R requires 64 RF paths with spacing between antennas is approx. 4.2 cm at given frequency of about 3.5 GHz.
- ➔ Due to more RF paths and antennas lot of power is dissipate.

## CHAPTER 3

### Pilots and Pilot Contamination

#### 3.1 Channel Estimation and the concept of Pilots

Channel estimation is crucial for massive multiple-input multiple-output (MIMO) systems to scale up multi-user (MU) MIMO, providing great improvement in spectral and energy efficiency. In all communication the signal goes through a medium (called channel) and the signal gets distorted or various noise is added to the signal while the signal goes through the channel. To properly decode the received signal without much errors are to remove the distortion and noise applied by the channel from the received signal. To do this, the first step is to figure out the characteristics of the channel that the signal has gone through. The technique/process to characterize the channel is called 'channel estimation'. This process would be illustrated as below.

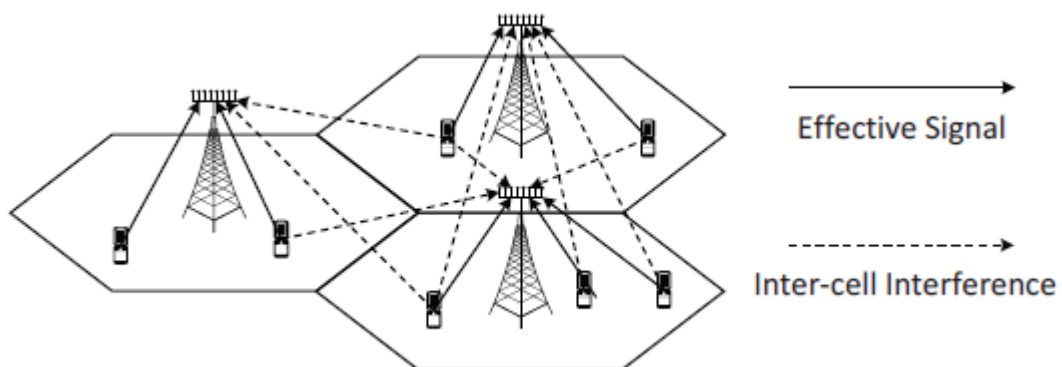


**Figure 3.1:-** Obtaining accurate channel state information (CSI) in multiuser MIMO.

There are many different ways for channel estimation, but fundamental concepts are similar. The process is done as follows.

- i) set a mathematical model to correlate 'transmitted signal' and 'received signal' using 'channel' matrix.
- ii) Transmit a known signal (we normally called this as 'reference signal' or 'pilot signal') and detect the received signal.

iii) By comparing the transmitted signal and the received signal, we can figure out each element of channel matrix.

Consider the wireless channel model:

Let  $x(k)$ ,  $y(k)$  be the  $k$ th transmitted and received pilot symbols respectively.  $n(k)$  is the additive white Gaussian noise and  $h$  is the Rayleigh fading channel coefficient.

$$y(k) = hx(k) + n(k) \quad (3.1)$$

The process of computing this channel coefficient  $h$  at the wireless receiver is termed channel estimation.  $h$  is defined as the fading channel coefficient. A popular scheme for estimating the wireless channel is through the transmission of pilot or training symbols. Pilot symbols are a predetermined fixed set of symbols which are transmitted over the wireless channel. This set of symbols is known to the wireless receiver as it is programmed beforehand. The receiver observes the outputs corresponding to the transmitted pilot symbols and with knowledge of the transmitted pilot symbols, proceeds to estimate the unknown fading channel coefficient.

### 3.2 Acquiring Channel State Information

The channel responses,  $h_{ijk}$ , are utilized by BS  $j$  to process the UL and DL signals. We have assumed so far that the channel responses are known perfectly, but in practice, these vectors need to be estimated regularly. More precisely, the channel responses are typically only constant for a few milliseconds and over a bandwidth of a few hundred kHz. A random distribution is commonly used to model the channel variations. The current set of channel response realizations is called the channel state and the knowledge that the BSs have of them is referred to as the channel state information (CSI). Full statistical CSI regarding the distributions of random variables is assumed to be available anywhere in the network, while instantaneous CSI regarding the current channel realizations need to be acquired at the same pace as the channels change. The main method for CSI acquisition is pilot signalling, where a predefined pilot signal is transmitted from an antenna. As illustrated in 3.2, any other antenna in the network can simultaneously receive the transmission and compare it with the known pilot signal to estimate the channel from the transmitting antenna. If we instead need to



estimate the channel response from two transmitting antennas, two orthogonal pilot signals are generally required to separate the signals from the two antennas. The orthogonality is achieved by spending two samples on the transmission. The number of orthogonal pilot signals is proportional to the number of transmit antennas, while any number of receive antennas can “listen” to the pilots simultaneously and estimate their individual channels to the transmitters.

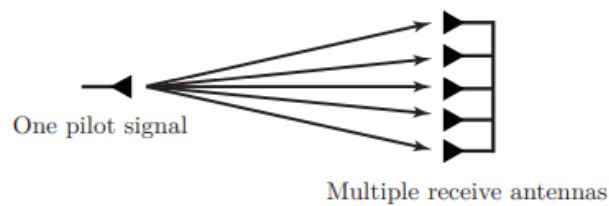


**Figure 3.2:-** When an antenna is transmitting a pilot signal, any number of receive antennas can simultaneously receive the pilot signal and use it to estimate their respective channels to the transmitter.

### 3.3 Coherence Time

The time during which the channel can be reasonably well viewed as time-invariant is called the coherence time and denoted by  $T_c$  (measured in seconds). To relate  $T_c$  to the characteristics of the physical propagation environment, we consider a simple two-path propagation model where a transmit antenna emits a signal  $x(t)$  that reaches the receiver both directly via a LoS path, and via a single specular reflection; see Figure 3.3(a).

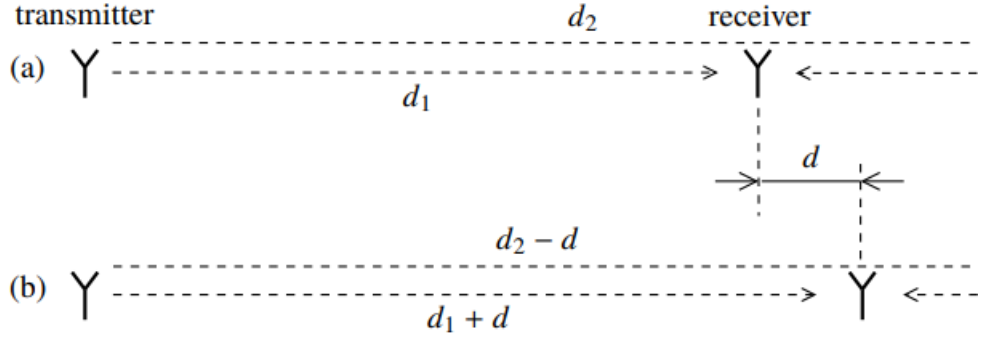


**Figure 3.3:-** Illustration of the two-path propagation model used to motivate the definitions of coherence time and coherence bandwidth.

If both paths have unit strength, and the bandwidth of  $x(t)$  is small enough that time-delays can be approximated as phase shifts, then by the superposition principle the received signal is

$$\begin{aligned}
 y(t) &= \left( e^{-i2\pi f c \frac{d_1}{c}} + e^{-i2\pi f c \frac{d_2}{c}} \right) x(t) \\
 &= \left( e^{-i2\pi \frac{d_1}{\lambda}} + e^{-i2\pi \frac{d_2}{\lambda}} \right) x(t)
 \end{aligned} \tag{3.2}$$

where  $d_1$  and  $d_2$  are the propagation path lengths defined in Figure 3.3(a).

Suppose, for the sake of argument, that when the receiver is located as shown in Figure 3.3(a),  $d_1/\lambda$  and  $d_2/\lambda$  are integers. Then the two paths add up constructively and  $y(t) = 2x(t)$ . Next, if the receiver is displaced  $d$  meters to the right, so that we have the situation in Figure 3.3(b), the received signal will instead be

$$\begin{aligned}
 y(t) &= \left( e^{-i2\pi \frac{d_1}{\lambda}} + e^{-i2\pi \frac{d_2}{\lambda}} \right) x(t) \\
 &= 2 \cos\left( 2\pi \frac{d}{\lambda} \right) x(t)
 \end{aligned} \tag{3.3}$$

The two paths add up destructively if the cosine in (3.3) is equal to zero. As shown in Figure 3.4(a), this occurs periodically for displacements  $d$  that are spaced  $\lambda/2$  meters apart. The channel may be considered time-invariant as long as the receiver does not

move farther than this distance,  $\lambda/2$ . This means that if the receiver moves with velocity  $v$  meters/second, then the coherence time,  $T_c$ , is

$$T_c = \frac{\lambda}{2v} \text{ seconds} \quad (3.4)$$

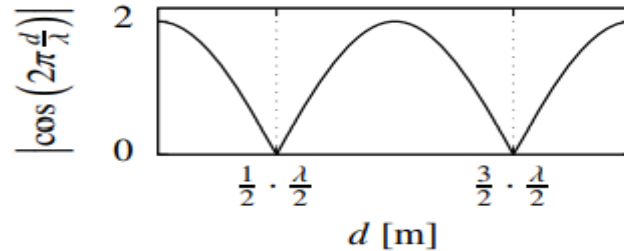


**Figure 3.4(a)**

(a) The coherence time,  $T_c$ , is the time it takes to move the distance between two consecutive locations at which the two paths add up destructively, that is,  $\lambda/2$  meter.

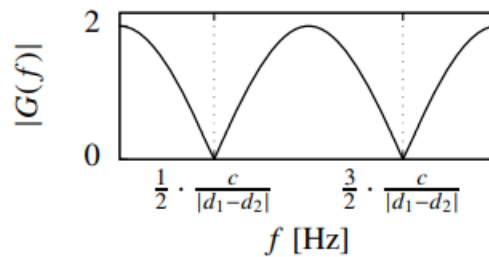


**Figure 3.4(b)**

(b) The coherence bandwidth,  $B_c$ , is the frequency separation between two nulls of the frequency response  $G(f)$ , that is,  $c/|d_1 - d_2|$  Hz.

**Figure 3.4:-** Definitions of coherence time and coherence bandwidth for the two-path model in Fig a and b.

### 3.4 Coherence Bandwidth

Consider now the transmission of a waveform whose time-duration is shorter than the coherence time,  $T_c$ . The relation between  $x(t)$  and  $y(t)$  is then

approximately time-invariant, and defined by the channel impulse response  $g(t)$  (where  $y(t) = \int_{-\infty}^{\infty} d\tau g(\tau)x(t - \tau)$ ) or, equivalently, by the channel frequency response

$$G(f) = \int_{-\infty}^{\infty} dt g(t)e^{-i2\pi ft} \quad (3.5)$$

Generally, the magnitude of the channel frequency response,  $|G(f)|$ , varies with  $f$ . The length of a frequency interval over which  $|G(f)|$  is approximately constant is called the coherence bandwidth and denoted by  $B_c$  (measured in Hz). Consider again the two-path propagation model in Figure 3.3(a), and assume that  $d_1$  and  $d_2$  are fixed and chosen such that  $d_1/\lambda$  and  $d_2/\lambda$  are integers. If a sinusoidal signal,  $x(t) = e^{i2\pi ft}$ , is transmitted, then the received signal is

$$y(t) = (e^{-i2\pi(fc+f)\frac{d_1}{c}} + e^{-i2\pi(fc+f)\frac{d_2}{c}})e^{-i2\pi ft} \quad (3.6)$$

Hence, the frequency response of the channel is

$$\begin{aligned} G(f) &= e^{-i2\pi(fc+f)\frac{d_1}{c}} + e^{-i2\pi(fc+f)\frac{d_2}{c}} \\ &= e^{-i2\pi f\frac{d_1}{c}} + e^{-i2\pi f\frac{d_2}{c}} \end{aligned} \quad (3.7)$$

The magnitude of the frequency response is

$$|G(f)| = |e^{-i2\pi f\frac{d_1}{c}} + e^{-i2\pi f\frac{d_2}{c}}| \quad (3.8)$$

independently of  $f_c$ .  $|G(f)|$  has zero-crossings at frequencies periodically spaced  $c/|d_1 - d_2|$  Hz apart; see Figure 3.4(b). Analogously to the definition of coherence time, we define the coherence bandwidth  $B_c$  to be the spacing between two nulls of  $|G(f)|$ , that is

$$B_c = \frac{c}{|d_1 - d_2|} \text{ Hz} \quad (3.9)$$

While the two-path model represents a simplified description of reality, in practice we expect  $|G(f)|$  to be substantially constant over a frequency interval whose length is given by (3.9), where  $|d_1 - d_2|$  is the maximum difference in length between different propagation paths from the transmitter to the receiver. As a first-order approximation,  $|d_1 - d_2|/c$  is equal to the delay spread of the channel, and  $g(t)$  is time-limited to  $|d_1 - d_2|/c$  seconds.

### 3.5 Coherence Interval

A time-frequency space of duration  $T_c$  seconds and bandwidth  $B_c$  Hz is called a coherence interval. This is the largest possible time-frequency space within which the effect of the channel reduces to a multiplication by a complex-valued scalar gain  $g$ . The magnitude  $|g|$  represents the scaling of the waveform envelope and  $\arg(g)$  represents the shift in its phase. According to the sampling theorem, any  $T$ -second segment of a waveform  $x(t)$  whose energy is substantially contained in a  $B$  Hz wide frequency interval can be described in terms of  $BT$  (complex-valued) samples taken at intervals of  $1/B$  seconds. This means that  $B_c T_c$  (complex-valued) samples are required to define a waveform that fits into one coherence interval. We therefore say that a coherence interval has the length

$$\tau_c = B_c T_c \text{ samples.}$$

### 3.6 TDD Coherence Interval Structure:-

TDD operation is ideal for Massive MIMO because the training burden is independent of the number of base station antennas. Throughout the book, we assume half-duplex TDD so that only one end of the link is transmitting at any one time, either the base station or the terminals. As a consequence, the coherence interval naturally divides into uplink and downlink subintervals, not necessarily of equal duration. Figure 3.5 illustrates two possible configurations, where Figure 3.5(a) includes provision for downlink as well as uplink pilots, and Figure 3.5(b) has only uplink pilots. Not shown are guard intervals between uplink and downlink transmissions.

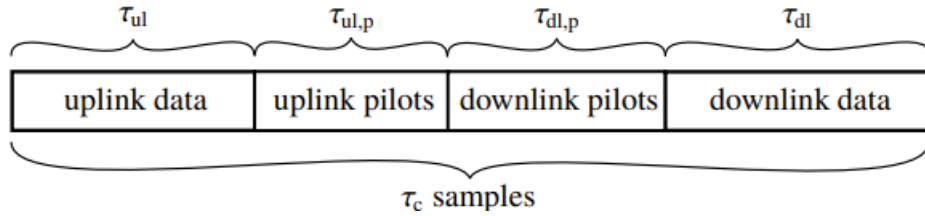
Let  $\tau_{ul}$  be the number of samples per coherence interval spent on transmission of uplink payload data,  $\tau_{ul,p}$  the number of samples per coherence interval spent on uplink pilots,  $\tau_{dl}$  the number of samples used for transmission of downlink payload data, and  $\tau_{dl,p}$  the number of samples allocated for downlink pilots. For the Figure 3.5(a) structure,

$$\tau_{ul} + \tau_{ul,p} + \tau_{dl,p} + \tau_{dl} = \tau_c \quad (3.10)$$

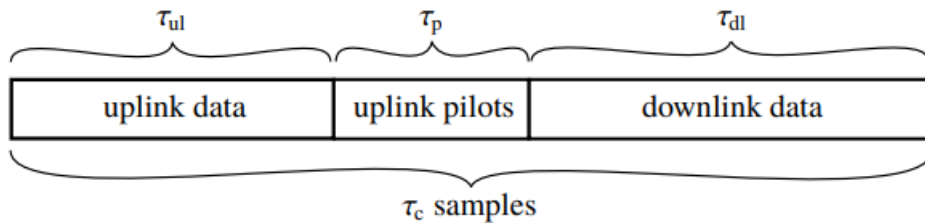
We show later that uplink pilots alone are sufficient to make TDD Massive MIMO work, and for the remainder of the book we assume the coherence interval structure of

Figure 3.5(b). For the sake of simplicity, we drop the subscript ul from the parameter  $\tau_{ul,p}$ , and the structural constraint becomes

$$\tau_{ul} + \tau_p + \tau_{dl} = \tau_c \quad (3.11)$$



(a) With downlink pilots



(b) Without downlink pilots

**Figure 3.5:-** Allocation of the samples in a coherence interval.

### 3.7 Coherence Block

A coherence block consists of a number of subcarriers and time samples over which the channel response can be approximated as constant and flat-fading. If the coherence bandwidth is  $B_c$  and the coherence time is  $T_c$ , then each coherence block contains  $\tau_c = B_c T_c$  complex-valued samples. The number of practically useful samples per coherence block can be smaller than  $B_c T_c$ .

The concepts of multicarrier modulation and coherence block are illustrated in Figure 3.7. The random channel responses in one coherence block are statistically identical to the ones in any other coherence block, irrespective of whether they are separated in time and/or frequency. Hence, the channel fading is described by a stationary ergodic random process.

The performance analysis is therefore carried out by studying a single statistically representative coherence block. We assume that the channel realizations are independent between any pair of blocks, which is known as a block fading assumption.

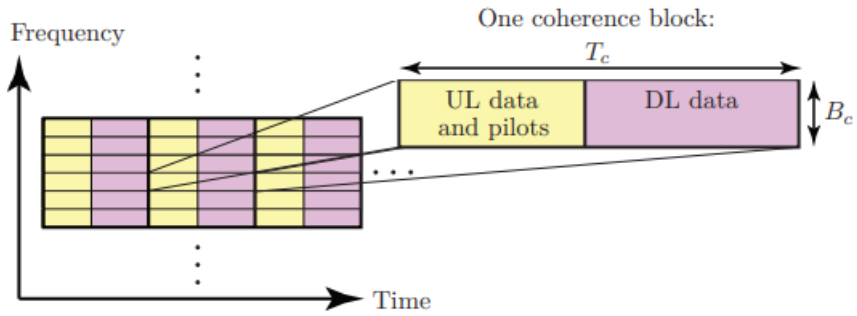


**Figure 3.6:-** The TDD multicarrier modulation scheme of a canonical Massive MIMO network. The time-frequency plane is divided into coherence blocks in which each channel is time-invariant and frequency flat.

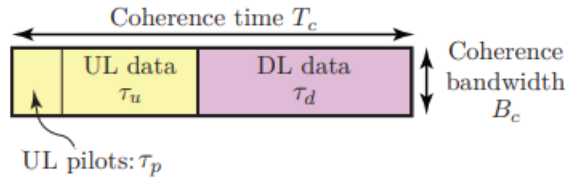


**Figure 3.7:-a)** The samples are used for UL pilots, UL data, and DL data.

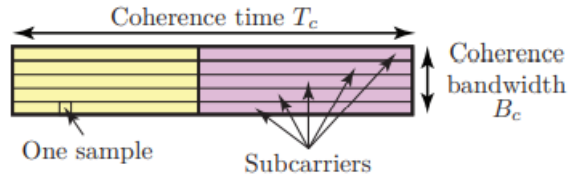


**Figure 3.7:- b)** The samples can belong to different subcarriers.

Each coherence block is operated in TDD mode and Figure 3.8 illustrates how the  $\tau_c$  samples are located in the time and frequency plane. The samples are used for three different things:

- 1)  $\tau_p$  UL pilot signals
- 2)  $\tau_d$  UL data signals
- 3)  $\tau_u$  DL pilot signals

The size of a coherence block is determined by the propagation environment, UE mobility, and carrier frequency. Each UE has an individual coherence bandwidth and coherence time, but it is hard to dynamically adapt the network to these values since the same protocol should apply to all UEs. A practical solution is to dimension the coherence block for the worst-case propagation scenario that the network

should support. If a UE has a much larger coherence time/bandwidth, then it does not have to send pilots in every block.

It is hard to give a precise dimensionality of the coherence block since it depends on many physical factors, but there is a common rule-of-thumb. The coherence time is the time interval over which the phase and amplitude variations in the channel due to UE mobility are negligible. This can be approximated as the time it takes to move a substantial fraction of the wavelength  $\lambda$ , say, a quarter of the wavelength:  $T_c = \lambda/4v$  where  $v$  is the velocity of the UE. Hence, the coherence time is inversely proportional to the carrier frequency and the channels need to be estimated less frequently in the conventional cellular frequency range of 1–6 GHz as compared to the mm Wave frequency range of 30–300 GHz. The coherence bandwidth is determined by phase differences in the multipath propagation. It can be approximated as  $B_c = 1/(2T_d)$  where  $T_d$  is the delay spread.

### **3.8 Need for Pilots**

The channel responses of  $h$  are utilized by the BS to process the UL and DL signals. We have assumed so far that the channel responses are known perfectly, but in practice, these vectors need to be estimated regularly.  $H$  has to be estimated at the receiver, prior to the beginning of the communication, so that information symbols can be decoded at the receiver and there's no error. Therefore, acquiring the channel state information is important for communication. The main method for CSI acquisition is pilot signaling, where a predefined pilot signal is transmitted from an antenna. To calculate the spectral efficiency, the possession of CSI is crucial. On uplink, the base station alone must know the channels, and each terminal has to be told its permissible transmission rate separately. On the downlink, both the base station and the terminals must have CSI. Since the pilot signal is known to the BS, it can compare the received pilots with the known pilot signal to estimate the channel.



### 3.9 Uplink Pilots and Channel Estimation

Learning the channel at the base station is a critical operation. As we have seen, a wideband channel can be decomposed into coherence intervals of duration  $T_c$  seconds and bandwidth  $B_c$  Hz. Every such interval offers  $\tau_c = B_c T_c$  independent uses of a frequency-flat channel. Figure 3.3(b) illustrates the three activities that occupy each coherence interval: uplink data transmission, uplink pilot transmission, and downlink data transmission. In every coherence interval, the terminals use  $\tau_p$  of the  $\tau_c$  available samples to transmit pilots that are known at both ends of the link, and from which the base station estimates the channels.

### 3.10 Orthogonal Pilots

Each coherence interval must host  $K$  pilot waveforms, and in order for them not to interfere, they have to be mutually orthogonal. Henceforth, we assume that the terminals are assigned mutually orthogonal pilot sequences of length  $\tau_p$ , where  $\tau_c \geq \tau_p \geq K$ . Any set of orthogonal pilots with the same energies yield the same performance. The significance of  $\tau_p$  is to quantify how much energy each terminal spends on pilots in each coherence interval. In principle, any  $\tau_p$  samples in the uplink part of the coherence interval can be used for pilots. In practice, transmitters are typically peak-power limited, so constant-modulus signals, such as orthogonal sinewaves, make ideal pilots. We assign the  $k$ th terminal a pilot sequence denoted by a  $\tau_p \times 1$  vector  $\phi_k$ , which is the  $k$ th column of a  $\tau_p \times K$  unitary matrix, such that  $\tau_p \geq K$  and  $\Phi^H \Phi = I_K$ .

### 3.11 Pilot Contamination

Since the channel coherence blocks are of limited size, it is necessary to reuse pilot sequences across cells. The inter-cell interference increases the estimation errors and also makes the channel estimates of two UEs that use the same pilot are correlated. This phenomenon is called pilot contamination.

UEs that transmit the same pilot sequence contaminate each other's channel estimates. The interference not only reduces the estimation quality, but also makes the channel estimates statistically dependent—although the true channels are

statistically independent. Pilot contamination has an important impact beyond channel estimation, since the contamination makes it particularly hard for the BS to mitigate interference between UEs that use the same pilot.

One word that is tightly connected with Massive MIMO is *pilot contamination*. This is a phenomenon that can appear in any communication system that operates under interference.

The base station wants to know the channel responses of its user terminals and these are estimated in the uplink by sending pilot signals. Each pilot signal is corrupted by inter-cell interference and noise when received at the base station. For example, consider the scenario illustrated below where two terminals are transmitting simultaneously, so that the base station receives a superposition of their signals—that is, the desired pilot signal is *contaminated*.

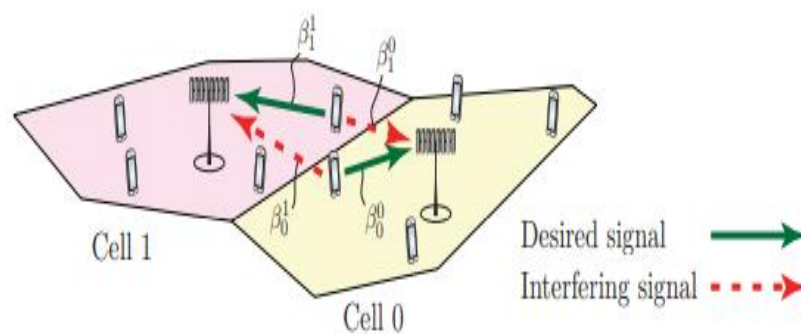


**Figure 3.8:-Pilot Contamination Illustration**

UEs that transmit the same pilot sequence contaminate each other’s channel estimates. The interference not only reduces the estimation quality (i.e., increases the MSE) but also makes the channel estimates statistically dependent—although the true channels are statistically independent. Pilot contamination has an important impact beyond channel estimation, since the contamination makes it particularly hard for the BS to mitigate interference between UEs that use the same pilot. Pilot contamination is often described as a main characteristic and limiting factor of Massive MIMO. The phenomenon is not unique to Massive MIMO, it exists in most cellular networks because of the practical necessity to reuse the time-frequency resources across cells. Pilot contamination can, however, have a greater impact on Massive MIMO than on

conventional networks. This is partially because the large number of UEs requires the pilot sequences to be reused more frequently in space and partially because the signal processing in Massive MIMO is particularly good at suppressing interference between UEs with orthogonal pilots.

When estimating the channel from the desired terminal, the base station cannot easily separate the signals from the two terminals. This has two key implications:

1. First, the interfering signal acts as coloured noise that reduces the channel estimation accuracy.
2. Second, the base station unintentionally estimates a superposition of the channel from the desired terminal and from the interferer.

Later, the desired terminal sends payload data and the base station wishes to coherently combine the received signal, using the channel estimate. It will then unintentionally and coherently combine part of the interfering signal as well.

This is particularly poisonous when the base station has  $M$  antennas, since the array gain from the receive combining increases both the signal power and the interference power proportionally to  $M$ . Similarly, when the base station transmits a beamformed downlink signal towards its terminal, it will unintentionally direct some of the signal towards the interferer.

## **3.12 System Model for Uplink and Downlink**

Having discussed about channel estimation, pilots and pilot contamination, now is the time to define a system model so as to follow up our project to find and compare methods that can mitigate pilot contamination.

### **3.12.1 Uplink**

The UL transmission in Massive MIMO is illustrated in Figure 3.10

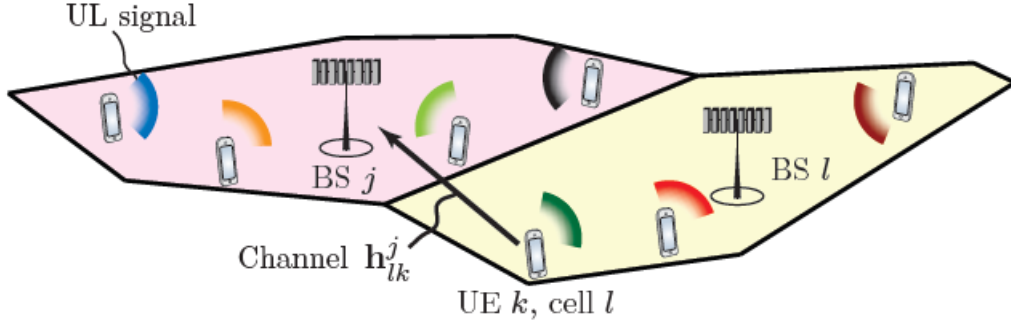


**Figure 3.9:-** Illustration of the UL Massive MIMO transmission in cell  $j$  and cell  $l$ .

The channel vector between BS  $j$  and UE  $k$  in cell  $l$  is called  $h_{lk}^j$ .

The received UL signal  $y_j$  at BS  $j$  is modelled

$$\begin{aligned}
 y_j &= \sum_{l=1}^L \sum_{k=1}^{K_l} h_{lk}^j s_{lk} + n_j \\
 &= \underbrace{\sum_{k=1}^{K_j} h_{jk}^j s_{jk}}_{\text{Desired signal}} + \underbrace{\sum_{l=1}^L \sum_{i=1}^{K_l} h_{li}^j s_{li}}_{\text{Intra-cell signals}} + \underbrace{n_j}_{\text{Noise}}
 \end{aligned} \quad (3.12)$$

Where  $n_j$  is independent additive receiver noise with zero mean and variance. The channels are constant within a coherence block, while the signals and noise take new realization at every sample. During data transmission, the BS in cell  $j$  selects the receive combining vector  $v_{jk} \in \mathbb{C}^{M_j}$  to separate the signal from its  $k$ th desired UE from the interference as

$$v_{jk}^H y_j = v_{jk}^H h_{jk}^j s_{jk} + \sum_{i=1}^{K_j} v_{jk}^H h_{ji}^j s_{ji} + \sum_{l=1}^L \sum_{i=1}^{K_l} v_{jk}^H h_{li}^j s_{li} + v_{jk}^H n_j \quad (3.13)$$

### 3.12.2 Downlink

The DL transmission in Massive MIMO is illustrated in Figure 3.9. The BS in cell  $l$  transmits the DL signal

$$X_l = \sum_{i=1}^{K_l} W_{li} s_{li} \quad (3.14)$$

Where the last term in the expression is the DL data signal intended for UE  $k$  in the cell which depends on the signal power.

The received signal  $y_{jk} \in \mathbb{C}$  at UE  $k$  in cell  $j$  is modelled as

$$\begin{aligned}
 y_{jk} &= \sum_{l=1}^L (h_{jk}^l)^H X_l + n_{jk} \\
 &= \sum_{l=1}^L \sum_{i=1}^{K_l} (h_{jk}^l)^H W_{li} s_{li} + n_{jk}
 \end{aligned}$$

$$=(h_{jk}^j)^H W_{jk} S_{jk} + \sum_{i=1}^{K_j} (h_{jk}^j)^H W_{ji} S_{ji} + \sum_{l=1}^L \sum_{i=1}^{K_l} (h_{jk}^l)^H W_{li} S_{li} + n_{jk} \quad (3.15)$$

Where, the independent additive white noise at the receiver is given by,

$$n_{jk} \sim N_c(0, \sigma_{DL}^2) \quad (3.16)$$

Thus, the term corresponding to inter-cell interference is due to the reuse of pilot sequences in adjacent cells, which worsens the channel estimate quality and thereby making it harder for precoding or decoding the information. Therefore, it is important that we mitigate the pilot contamination that is being caused by the reuse of pilot sequences by obtaining and implementing proper pilot allocation methods, which will be discussed in the next chapter.

## CHAPTER 4

### Methods to Mitigate Pilot Contamination

#### 4.1 Introduction to Pilot Contamination

Massive MIMO has been recognized as a promising technology to meet the demand for higher data capacity for mobile networks. Although promising, each base station needs accurate estimation of the channel state information CSI, either through feedback or channel reciprocity schemes in order to achieve the benefits of massive MIMO in practice. Time division duplex TDD has been suggested as a better mode to acquire timely CSI in massive MIMO systems. The use of non-orthogonal pilot schemes, proposed for channel estimation in multi-cell TDD networks, is considered as a major source of pilot contamination in the literature due to the limitations of coherence time. The limited time-slot resources i.e. the coherent interval restricts the number of available pilot sequences for conducting the channel estimation. Accordingly, the necessary pilots reuse among cells unavoidably results in the serious pilot contamination problem. The reuse of pilot sequences in a Massive MIMO system leads to pilot contamination, which reduces the channel estimation quality and adds coherent interference in the data transmission.

The number of available orthogonal pilot sequences is limited by the size of the coherence block. Therefore, pilots need to be reused among cells in practical networks. This causes interference in the channel estimation process that, in turn, adds coherent interference in the UL and DL data transmissions, giving rise to the so-called pilot contamination effect.

#### 4.2 Conventional Pilot Allocation Scheme

If the system model consists of  $L$  cells, where in each of them a BS with  $M$  antennas is serving  $K$  single-antenna users. If we consider that there are  $\tau_p$  pilot sequences can be distributed among the UEs and reused across cells in different ways. Unless stated otherwise, we consider  $\tau_p = fK$  pilots, with the integer  $f$  being called the

pilot reuse factor. This means that there are  $f$  times more pilots than UEs per cell and the same subset of pilots is reused in a fraction  $1/f$  of the cells. We consider  $f \in \{1, 2, 4\}$  in the running example and the corresponding reuse patterns are illustrated in Figure 4.1. The cells that use the same pilots are said to belong to the same pilot group. The pilots are randomly assigned to the UEs in every cell in the sense that the  $k$ th UE in two cells, that belong to the same pilot group, uses the same pilot. This is called random pilot allocation scheme, which is the default pilot allocation employed amongst all the cells. Random pilots lead to pilot contamination.

For each realization of the random pilots, you will get a set of pilot sequences that is either orthogonal or non-orthogonal. Then the pilot contamination effect follows in the same way as for deterministic pilots. The potential benefit of having random pilots is that you can “share” the pilot contamination between the users, so that everyone gets an equal share on average. However, since cell-edge users are more sensitive to pilot contamination than cell-center users, you might want to coordinate the pilot allocation across cells instead of randomize it. In that sense, random pilots are the baseline scheme that any “smart” scheme should be able to beat. So, we need methods that are able to mitigate the pilot contamination vastly that perform better than this random pilot allocation.

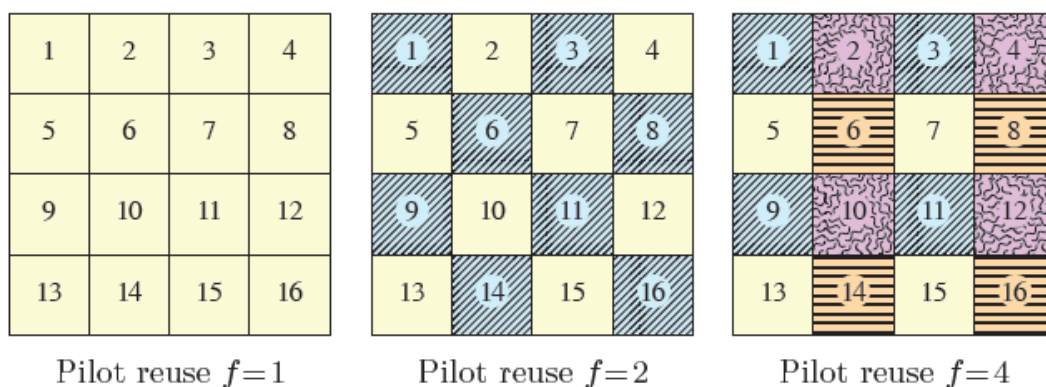


**Figure 4.1:-** Examples of pilot reuse factors

### **4.3 Approaches to Mitigate Pilot Contamination**

Many researchers have analyzed pilot contamination over the six years that have passed since Marzetta uncovered its importance in Massive MIMO systems. We now have a quite good understanding of how to mitigate pilot contamination. There is a plethora of different approaches, whereof many have complementary benefits. If pilot contamination is not mitigated, it will both reduce the array gain and create coherent interference. Some approaches mitigate the pilot interference in the channel estimation phase, while some approaches combat the coherent interference caused by pilot contamination. In our literature survey we have discovered a few methods and approaches to mitigate PC.

#### **4.3.1 Data-aided Channel Estimation**

Another approach is to “decontaminate” the channel estimates from pilot contamination, by using the pilot sequence and the uplink data for joint channel estimation. This has the potential of both improving the estimation quality leading to a stronger desired signal) and reducing the coherent interference. Ideally, if the data is known, data-aided channel estimation increase the length of the pilot sequences to the length of the uplink transmission block. Since the data is unknown to the receiver, semi-blind estimation techniques are needed to obtain the channel estimates.

Recent work has proved that one can fully decontaminate the estimates, as the length of the uplink block grows large, but it remains to find the most efficient semi-blind decontamination approach for practical block lengths.

#### **4.3.2 Pilot Assignment and Dimensioning**

Which subset of users that share a pilot sequence makes a large difference, since users with large pathloss differences and different spatial channel correlation cause less contamination to each other. Recall that higher estimation quality both increases the gain of the desired signal and reduces the coherent interference. Increasing the number of orthogonal pilot sequences is a straightforward way to decrease the contamination, since each pilot can be assigned to fewer users in the network. The price to pay is a larger pilot overhead, but it seems that a reuse factor of



3 or 4 is often suitable from a sum rate perspective in cellular networks. The joint spatial division and multiplexing (JSDM) provides a basic methodology to take spatial correlation into account in the pilot reuse patterns.

Alternatively, pilot sequences can be superimposed on the data sequences, which gives as many orthogonal pilot sequences as the length of the uplink block and thereby reduces the pilot contamination. This approach also removes the pilot overhead, but it comes at the cost of causing interference between pilot and data transmissions. It is therefore important to assign the right fraction of power to pilots and data. A hybrid pilot solution, where some users have superimposed pilots and some have conventional pilots, may bring the best of both worlds. If two cells use the same subset of pilots, the exact pilot-user assignment can make a large difference. Cell-center users are generally less sensitive to pilot contamination than cell-edge users, but finding the best assignment is a hard combinatorial problem. There are heuristic algorithms that can be used and also an optimization framework that can be used to evaluate such algorithms.

### **4.3.3 Multi-cell Cooperation**

A combination of network MIMO and macro diversity can be utilized to turn the coherent interference into desired signals. This approach is called pilot contamination precoding by Ashikhmin et al. and can be applied in both uplink and downlink. In the uplink, the base stations receive different linear combinations of the user signals. After maximum ratio combining, the coefficients in the linear combinations approach deterministic numbers as the number of antennas grow large. These numbers are only non-zero for the pilot-sharing users. Since the macro diversity naturally creates different linear combinations, the base stations can jointly solve a linear system of equations to obtain the transmitted signals. In the downlink, all signals are sent from all base stations and are precoded in such a way that the coherent interference sent from different base stations cancel out. While this is a beautiful approach for mitigating the coherent interference, it relies heavily on channel

hardening, favorable propagation, and Rayleigh fading. It remains to be shown if the approach can provide performance gains under more practical conditions.

#### **4.4 Methods to Mitigate Pilot Contamination**

In our project, we have worked on a few existing methods to mitigate pilot contamination which occurs due to the reuse of an orthogonal pilot signal in an adjacent neighboring cell, leading to interference of channel state information at the base station of the desired cell.

##### **4.4.1 Methods taken into Consideration**

In the literature survey, after looking at multiple methods, two intuitive methods have been chosen to mitigate pilot contamination and they are

- 1) Soft Pilot Reuse Scheme followed by Weighted Graph Coloring
- 2) A New Strategy Based on Large Scale Fading Coefficients

The two methods have been studied thoroughly and compared to find out the better method to mitigate pilot contamination in terms of lower complexity and feasibility.

##### **4.4.2 Soft Pilot Reuse Scheme and Weighted Graph Coloring Method**

A novel pilot decontamination scheme based on two existing schemes (soft pilot reuse and weighted-graphed-coloring based pilot decontamination) is proposed. All users are firstly separated into two categories: cell centered users that reuse the same pilot sequences and cell edged users that use other orthogonal pilot subgroups to get rid of the severe contamination. But the slight contamination among the cell centered users still exists.

Then, in order to improve the decontamination of cell centered users, a weighted-graph-based method is applied. With such combination, the proposed scheme is able to mitigate the contamination and improve the quality of communication significantly.

Since CE requires pilot resources while the resources are limited but should be reused in multicell scenarios which results in PC, a modified pilot reuse scheme to mitigate PC is also necessary. Pilot sequences are designed to be orthogonal to each other and assigned for both single cell and neighbor cell, so that the interference

only occurs between cells. Allocation schemes based on coloring graph and weighted coloring graph (WGC-PD) are proposed previously. Those methods not only can reduce PC, but also achieve large uplink rate. In addition, a kind of pilot reuse scheme so called Soft Pilot Reuse Scheme (SPRS) is proposed, in which the users are separated into two categories: cell centered users and cell edged users. The cell centered users (likely subjected to slight PC) can use the same pilot resource while the cell edged users (likely subjected to serious PC) in adjacent cells apply other cell edge pilot subgroups, which probably enables to promote the pilot decontamination due to the orthogonality. A novel pilot decontamination scheme based on SPRS and WGC-PD is proposed in this paper. In the proposed scheme, SPRS is firstly applied to divide users and cells generally, then the focus is on the pilot decontamination among the cell centered users, and WGC-PD is applied to solve this problem more thoroughly than the previous solutions so that the performance is better in uplink massive MIMO.

An uplink multicell MIMO system is considered. The system includes  $J$  cells. Each cell has a BS which is loaded with  $N$  antennas providing service to  $K$  ( $K \ll N$ ) single antenna users. The channel impulse response vector connecting the  $k$ -th user in the  $j$ -th cell to the BS of the  $i$ -th cell can be written as

$$\mathbf{h}_{ijk} = \mathbf{g}_{ijk} \sqrt{\beta_{ijk}} \quad (4.1)$$

where,  $\beta_{ijk}$  denotes the large-scale fading coefficients which change slowly and can be easily tracked.

$\mathbf{g}_{ijk} \sim CN(0, \mathbf{I}_M)$  denotes the small-scale fading coefficients. Also,  $\beta_{ijk}$  is given by,

$$\beta_{i,j,k} = \frac{z_{i,j,k}}{\left(\frac{r_{i,j,k}}{R}\right)^\alpha} \quad (4.2)$$

$T$  out of  $T_c$  is used to transmit the  $P$  orthogonal uplink pilot sequences,  $\Phi_k \in \mathbb{C}^{T \times 1}$  for  $k=1,2,3,\dots,P$ . Then, we can have the matrix  $\Phi \in \mathbb{C}^{P \times T}$  to represent the  $P$  pilot sequences as  $\Phi = [\phi_1 \ \phi_2 \ \dots \ \phi_P]^T$ .

Where,  $\Phi^* \Phi^H = \mathbf{I}_P$ , and  $H$  is the Hermitian operator, which is a complex square matrix that is equal to its own conjugate transpose.

To obtain the Channel State Information, pilot signals are transmitted from the UEs prior to the transmission of original message signals. Then, the received pilot sequence  $Y_i^P \in \mathbb{C}^{M \times T}$  at the BS in the  $i$ -th cell can be represented as,

$$Y_t^p = \sqrt{\rho_p \sum_{j=1}^L \sum_{k=1}^K h_{ijk} \phi_k^T + N_i^p} \quad (4.3)$$

Where  $\rho_p$  denotes the pilot transmission power and the additive term is the noise (Additive White Gaussian Noise AWGN). Similarly, the received user data  $y_i^u \in \mathbb{C}^{M \times 1}$  at the BS in the  $i$ -th cell is,

$$y_i^u = \sqrt{\rho_u \sum_{j=1}^L \sum_{k=1}^K h_{ijk} x_{jk}^u + n_i^u} \quad (4.4)$$

Where  $x_{jk}^u$  denotes the symbol from the  $k$ -th user in the  $j$ -th cell,  $\rho_u$  denotes the uplink data transmission power and  $n_i^u$  is the AWGN vector. The channel estimate of the  $k$ -th user in the  $i$ -th cell can be represented as

$$h_{ijk} = \frac{1}{\sqrt{\rho_p}} Y_i^p \phi_k^H = \sum_{j=1}^L h_{ijk} + v_{ik} \quad (4.5)$$

Where  $v_{ik}$  denotes the equivalent noise.

The uplink SINR for the user of interest can be represented as,

$$SINR_{ik}^u = \frac{|h_{iik}^H h_{iik}|^2}{\sum_{j \neq i} |h_{iik}^H h_{iik}|^2 + \frac{|\varepsilon_{ik}^u|^2}{\rho_u}} \xrightarrow{M \rightarrow \infty} \frac{\beta_{iik}^2}{\sum_{j \neq i} \beta_{ijk}^2} \quad (4.6)$$

Where  $\varepsilon_{ik}^u$  denotes the corresponding interference which can be reduced to an arbitrarily low level by increasing the number of transmit antennas  $M$  at the BS. Thus, the corresponding average uplink capacity of this user can be calculated as

$$C_{ik}^u = E\{\log_2(1 + SINR_{ik}^u)\} \quad (4.7)$$

In summary, the PC caused by the reuse of the same orthogonal pilot group in adjacent cells cannot be reduced by increasing the number of antennas at the BS, hence it limits the achievable performance of multi-cell multi-user LS-MIMO systems.

#### 4.4.2.1 Soft Pilot Reuse

Based on the large-scale fading ( $\beta_{ijk}$ ) the users in each cell can be classified into two groups according to the following rules.

$$\begin{cases} \beta_{i,i,k}^2 > \rho_i: \text{Inner region users} \\ \beta_{i,i,k}^2 \leq \rho_i: \text{Outer region users} \end{cases} \quad (4.8)$$

where the grouping threshold for the  $i$ -th cell  $\rho_i$  can be defined as

$$\rho_i = \frac{\lambda}{K} \sum_{k=1}^K \beta_{i,i,k}^2 \quad (4.9)$$

And  $\lambda$  is adjustable according the real configuration. A simple example of the division is illustrated in Fig. 4.3

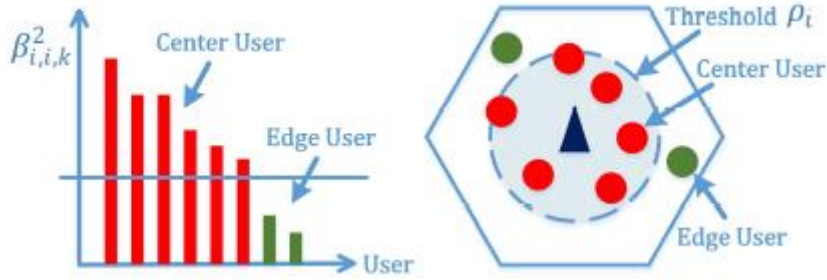


**Figure 4.2:-** An illustration of user's division in Soft pilot reuse scheme

Therefore, we introduce the SPRS in which the whole orthogonal pilot resource set is divided into two subsets, assigning to the cell edged users and cell centered users respectively. Furthermore, the latter is reused by cell centered users in all cells. Consider a typical MIMO system, which is composed of  $L$  hexagonal cells, where the  $i$ -th cell supports  $K_i$  users. The number of orthogonal pilot sequences required can be calculated as

$$K_{CS} = \max [ K_i, i=1,2,\dots,L ] \quad (4.10)$$

In contrast to the conventional MIMO scheme, where all users are treated identically, the  $K_i$  users of the  $i$ -th cell are firstly divided into two groups according to their large-scale fading coefficients ( $\beta_{ijk}$ ) which have cardinalities of

$$K_i = K_{i,c} + K_{i,e} \quad (4.11)$$

Where  $K_{i,c}$  denotes the number of center users, and  $K_{i,e}$  denotes the number of edge users. Thus, the number of orthogonal pilot sequences needed in the proposed SPR scheme can be calculated as

$$K_{SPR} = K_c + K_e \quad (4.12)$$

Where  $K_c = \max\{K_{i,c}, i=1,2,3,\dots,L\}$  denotes the number of pilot sequences assigned to center users. While  $K_e$  is the summation of all the edge users in all cells ( $\sum K_{i,e}$ ), denotes the number of pilot sequences assigned to the edge users. If the entire set of pilot sequences available is  $\Phi_{SPR}$ , then this set can be divided into

$$\Phi_{SPR} = [\Phi_{SPR}]^T \quad (4.13)$$

Where  $\Phi_c$  is reused for the center users in all cells and  $\Phi_e$  is applied to the edge users of the adjacent cells. Furthermore,  $\Phi_e$  can be divided into  $L$  partitions, as

$$\Phi_e = [\Phi_{e,1}^T \Phi_{e,2}^T \dots \dots \Phi_{e,L}^T]^T \quad (4.14)$$

Where  $\Phi_{e,i}$  is applied to the  $K_{i,e}$  edge users in the  $i$ -th cell. Thus, the pilot sequences applied to edge users are orthogonal to those of the other users roaming in the adjacent cells.

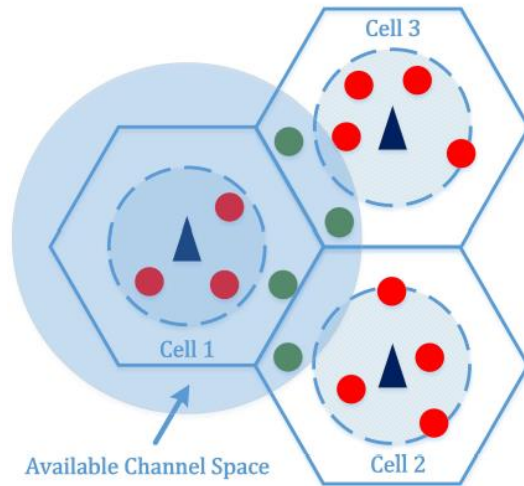


**Figure 4.3:-** The Soft pilot reuse scheme

So, since the pilot sequences in the single cell are orthogonal to each other and therefore no PC exists, and the cell edged users are free from very severe PC due to SPRS, the achievable decontamination mainly comes from eliminating the interference among different cell centered users reusing the same pilot resource. We firstly introduce a variable which is used to measure the intensity of the PC between any two users, which is given in the weighted graph coloring method below.

#### 4.4.2.2 Weighted Graph Coloring Method

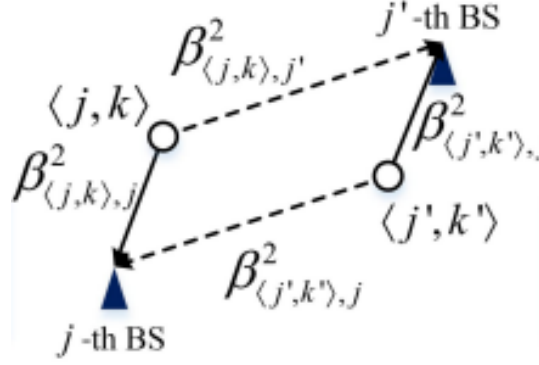


**Figure 4.4:-** Potential ICI: the ratio of interference channel strength and effective channel strength

In this method, as mentioned earlier, we define a variable to measure the intensity of PC (Pilot Contamination) between any 2 users, based on the large-scale fading coefficients.

Consider 2 users from 2 different cells as shown in the Fig. 4.5. User 1 is denoted by  $u(j,k)$  from the  $j$ th cell and user 2 is denoted by  $u(j',k')$  from the  $j'$ th cell. If both the users use the same pilot sequence, then arises the pilot contamination and the intensity of that PC is given by,

$$\zeta_{i,k}^{j,k'} = \frac{\beta_{i,j,k'}^2}{\beta_{i,i,k}^2} + \frac{\beta_{j,i,k}^2}{\beta_{j,j,k'}^2} \quad (4.15)$$

The larger this value is, the more serious PC will take place between these two users when the same pilot resource is reused by them. And mathematically, the MIMO interference can be translated as a graph theory problem:  $WG = (U,W)$ , where  $U$  represents the total users and  $W$  denotes the potential PC among them which is measured by (4.18). In this method,  $U$  and  $W$  only adapt to the cell centered users. To achieve the reduction of PC and the high rate of uplink transmission, the WGC-PD is introduced. The main idea of the WGC-PD is based on greedy algorithm in which the larger the weight  $W$  is, the prior these two users are assigned with pilot sequences to achieve the minimum PC.

The steps incorporated in this method are:

1) Initialization: Firstly, two users in different cells with the largest weighted-edge in the EWIG are selected. These two users are assigned with 2 different orthogonal pilots. Then they are added to the assigned set. This process continues for all users in a sequential way.

2) User Selection: The users are selected in the order of their weight sum of the edges connecting the user and the users in other cells within pilot set. Then the user with the largest potential PC will be selected and given pilot preferentially.

3) Pilot Assignment: Thus, the users/vertices are sorted in a descending fashion based on their weight sum connecting other users in different cells. And the pilots are assigned in that order so that the most severe PC causing user is assigned a pilot first and the user having least severity is also assigned a pilot finally.

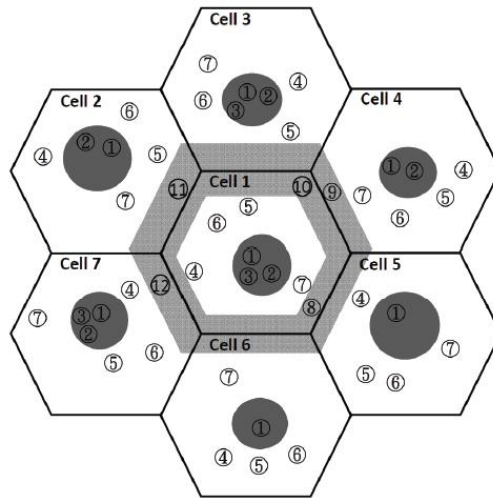


**Figure 4.5:-** WGC+SPRS scheme illustration in cells

The Algorithm in the next sub section summarizes the procedures of the proposed WGC-SPR scheme under two assumptions, i.e. 1)  $P < K$  and 2) the first cell i.e. ( $i = 1$ ) is the center cell. Therein, Lines 2-3 initialize some parameters. Lines 5-16 are to



categorize the users into the inner and outer region groups i.e. the  $K_{c,i}$  and  $K_{e,i}$ , respectively) based on the large scale fading coefficient and the grouping threshold. therein, Line 8 calculates the  $\rho_i$  using equation 4.12 for the all cells. Lines 17-33 are to further divide the outer region users into the hazard- and secure-edge region users (i.e. the  $K_{h,i}$  and  $K_{s,i}$ , respectively) according to the large scale fading coefficients  $\alpha_{i,1}$ , respectively. Lines 34-44 allocate the proper numbers of the orthogonal pilots to the inner, hazard- and secure-edge regions; therein, Lines 35 and 40 (including Line 47) adjust the  $\lambda$  and  $\lambda'$  to have proper values of the parameters mentioned such that the sum data rate can be maximized under the condition of  $P < K$ . Lines 45 applies the conventional WGC algorithm to reuse the pilots allocated to the secure-edge regions. At last, Line 46 calculates the achievable sum data rate  $R$ , and Line 50 decides the optimal values of  $\lambda^*$  and  $\lambda'^*$  as well as the optimal pilot allocations so that the sum data rate can be maximized.

#### 4.4.2.3 Algorithm for SPRS+WGC-PD

```

1: Initialization:
2:    $K'_{c,i} = K'_{e,i} = K_{s,i} = K_{h,i} = 0$ ;
3:    $\mathbb{K}_{c,i} = \mathbb{K}_{e,i} = \mathbb{K}_{s,i} = \mathbb{K}_{h,i} = \emptyset$ ;
4: Output:
5: for  $\lambda \in [\lambda_{\min} \lambda_{\max}]$  do
6:   for  $\lambda' \in [\lambda'_{\min} \lambda'_{\max}]$  do
7:     for  $i \in L$  do
8:       Obtain  $\rho_i$  by calculating (14);
9:       for  $k \in K$  do
10:        if  $\beta_{i,i,k}^2 > \rho_i$  then
11:           $\mathbb{K}_{c,i} = \mathbb{K}_{c,i} \cup u_{i,k}$ ;  $K'_{c,i} = K'_{c,i} + 1$ ;
12:        else
13:           $\mathbb{K}_{e,i} = \mathbb{K}_{e,i} \cup u_{i,k}$ ;  $K'_{e,i} = K'_{e,i} + 1$ ;
14:        endif
15:      end for
16:    end for
17:    for ( $i \in L$  and  $i \neq 1$ ) do
18:      Obtain  $\delta_{1,i}$  and  $\delta_{i,1}$  by using (38) and (40);
19:      for  $k \in K'_{e,1}$  do
20:        if  $\beta_{1,i,k}^2 > \delta_{1,i}$  then
21:           $\mathbb{K}_{h,1} = \mathbb{K}_{h,1} \cup u_{1,k}$ ;  $K_{h,1} = K_{h,1} + 1$ ;
22:        else
23:           $\mathbb{K}_{s,1} = \mathbb{K}_{s,1} \cup u_{1,k}$ ;  $K_{s,1} = K_{s,1} + 1$ ;
24:        endif
25:      end for
26:      for  $k \in K'_{e,i}$  do
27:        if  $\beta_{1,i,k}^2 > \delta_{i,1}$  then
28:           $\mathbb{K}_{h,i} = \mathbb{K}_{h,i} \cup u_{i,k}$ ;  $K_{h,i} = K_{h,i} + 1$ ;
29:        else
30:           $\mathbb{K}_{s,i} = \mathbb{K}_{s,i} \cup u_{i,k}$ ;  $K_{s,i} = K_{s,i} + 1$ ;
31:        endif
32:      end for
33:    end for
34:    if  $P < \max_i [K'_{c,i}]$  then
35:       $\lambda' = \lambda' + \Delta_{\lambda'}$ ; Go to 8;
36:    else
37:      Allocate  $\max_i [K'_{c,i}]$  orthogonal pilots to  $\Phi_c$ ;
38:    endif
39:    if  $P \leq \max_i [K'_{c,i}] + \sum_{i=1}^L K_{h,i}$  then
40:       $\lambda' = \lambda' + \Delta_{\lambda'}$ ; Go to 8;
41:    else
42:      Allocate  $\sum_{i=1}^L K_{h,i}$  orthogonal pilots to  $\Phi_h$ ;
43:      Allocate  $P - \max_i [K'_{c,i}] - \sum_{i=1}^L K_{h,i}$  orthogonal pilots to  $\Phi_s$ ;
44:    endif
45:    Apply the WGC scheme to reuse  $\Phi_s$  and obtain the pilot allocation  $\mathcal{P}_s$  for the secure-edge regions;
46:    Calculate (12) to obtain  $\mathcal{R}(\lambda, \lambda', \Phi_c, \Phi_h, \mathcal{P}_s)$ ;
47:     $\lambda = \lambda + \Delta_{\lambda}$ ;  $\lambda' = \lambda' + \Delta_{\lambda'}$ ;
48:  end for
49: end for
50:  $[\lambda^*, \lambda'^*, \Phi_c^*, \Phi_h^*, \mathcal{P}_s^*] = \arg \max_{\lambda, \lambda', \Phi_c, \Phi_h, \mathcal{P}_s} \mathcal{R}$ ;

```

#### 4.4.2.4 WGC+SPR Scheme Outline and Summary

The WGC-SPR scheme to effectively alleviate the pilot contamination caused by extensively reusing the pilots. And, accordingly, the uplink sum data rate can be remarkably improved for the multi-cell massive MIMO systems.

The time complexities of individual schemes are found out to be:

SPR	WGC	SPR+WGC
$\mathcal{O}(MN_\lambda(K_e^2 + K_c^2))$	$\mathcal{O}(P(KL)^3)$	$\mathcal{O}((P(N_\lambda N_{\lambda'} L^3 K^2 K_e)))$

In principle, the proposed WGC-SPR scheme extends the concept of the conventional SPR scheme to further divide the outer regions of the neighboring cells into the hazard- and secure-edge regions. Then, as implied by the name, the pilots allocated to the hazard-edge regions can't be reused, while the pilots belonging to the secure edge regions can be reused by utilizing the conventional WGC scheme. With properly designed hazard and secure edge regions, the proposed scheme can successfully suppress the increment of interference incurred by pilot reuse

#### 4.4.3 Strategy based on Large Scale Fading Coefficients

This method aims to address the problem of Pilot Contamination (PC) within Massive MIMO systems. The Strategy is mainly derived from the asymptotic regime, where Base Stations (BSs) are equipped with a large number of antennas. Regarding the fact that the available pilot resources are limited and many users should be assigned with pilots, the reuse of the same pilots within different cells is essential. Accordingly, the pattern where pilots are reused within different cells is considered herein. Specifically, the large-scale fading coefficients (LSFs) are exploited to show that the PC upon users depends on the distance between users that employ the same pilots. Hence, instead of optimizing the manner where pilots are assigned to users, the proposed method assigns pilots to users of different cells based on their LSF coefficients and through the exploitation of a simple matrix arrangement.

Instead of the previous presented methods (and references therein) that focus their studies on optimizing specific or multiple metrics, which lead sometimes to a high level of complexity, and the problem of convergence is a common issue that degrades the effectiveness of many techniques of optimization. However, in the present method, we propose a new optimization approach to overcome the problem of PC.

Specifically, the contribution of this method is as follows:

- 1) We derive a new decontaminating algorithm, which is based on the matrix analysis.
- 2) Instead of sharing information between BSs -which lead to the problem of backhaul signalling - the proposed algorithm requires only to share the LSF coefficients with a hub connected to all BSs (i.e. one network hub connected to a set of seven cells).
- 3) Simulation results prove the effectiveness of our proposal compared to both the Conventional Strategy (CS) which is the random allocation and the Weighted Graph Colouring (WGC) + Soft Pilot Reuse (SPR).

#### 4.4.3.1 The Proposed Algorithm

Compared to SSF coefficients, LSF coefficients varies more slowly. Accordingly, LSF coefficients can be easily tracked and shared by BSs instead of SSF coefficients that vary quickly. Accordingly, it is obvious to note that, the strategies which are designed based on LSF coefficients are desired and considered more powerful than the strategies which are based on SSF coefficients. Hence, the proposed algorithm exploits the fact that the users' LSF coefficients depend on the distance between users and BSs. Owing from that, each BS can classify its supported users based on their LSF coefficients. Let consider the LSF coefficient of a user  $k$  wandering in cell  $j$  to its supported BS of the same cell  $j$ . This coefficient can be expressed as in as follow:

$$\beta_{i,j,k} = \frac{z_{i,j,k}}{\left(\frac{r_{i,j,k}}{R}\right)^\alpha} \quad (4.16)$$

Where  $z_{j,i,k}$  is a log-normal distribution, and it follows a Gaussian distribution of a zero-mean and having a standard deviation  $\sigma_{\text{shadow}}$  and accounts for shadowing,  $r_{j,i,k}$  is the distance between the  $k$ th user and the BS of the  $j^{\text{th}}$  cell,  $R$  is the cell radius, and  $\alpha$  accounts for the path loss.

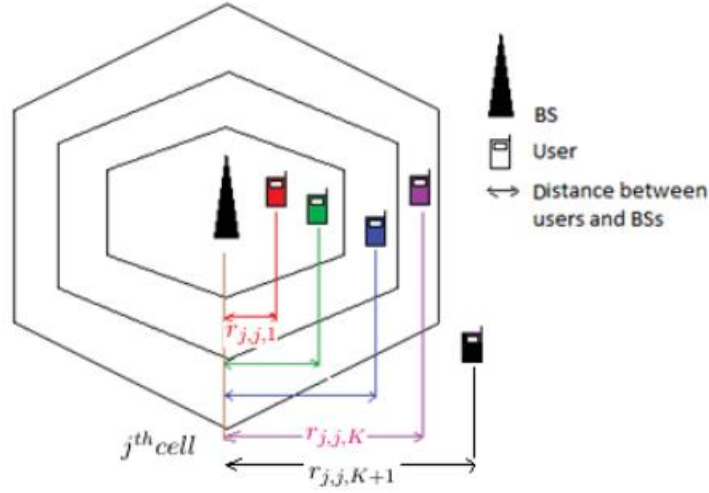


**Fig. 4.6:-** Users classification based on their LSF coefficients

Based on Interference Reduction in multi cell massive MIMO Systems, the size of user's LSF coefficients increases from the edge to the centre of a cell (Fig.4.7). Accordingly, BSs can classify their corresponding users in a vector through exploiting the LSF coefficients. It is important to note that the number of users per cell is the same (i.e.  $K$  user per cell). Let consider the example depicted at Fig.4.7, where the BS of the  $j^{\text{th}}$  cell classifies its supported users in a matrix of classification labelled  $\beta_j$ , and the  $(K + 1)^{\text{th}}$  user is considered out of the interest of the  $j^{\text{th}}$  BS. Hence,  $\beta_j$  can be expressed as follows:

$$\beta_j = [\beta_{j,j,1}^2, \dots, \beta_{j,j,k}^2, \dots, \beta_{j,j,K}^2] \quad (4.17)$$

In the second step, all BSs send their constructed matrices of classification  $\beta_j : j = 1, 2, \dots, L$  to a network hub, which is charged to construct a global matrix of classification, which can be expressed as follows:

$$\beta = [\beta_1^T, \dots, \beta_j^T, \dots, \beta_L^T] \quad (4.18)$$

From Fig.4.8 and based on the proof, the problem of PC diminishes when the distance between users that employ the same pilots is large. Accordingly, the proposed algorithm assigns different pilot sequences to users who are close to each other, this through the following proposition : Proposition: Let  $P \in C^{(L) \times K}$  be the pilot assignment matrix of the users of all cells (i.e  $L$  cell) and  $S = [\varphi[1], \varphi[2], \dots, \varphi[K]] \in$

$C^{\tau \times K}$  is a set of pilot sequences of length  $\tau$  and contain at least  $K$  pilots. Hence, the rows of  $P$  can be expressed for a cluster of 7 hexagonal cells as follows:

$$P(i, k = 1, 2, \dots, K)_{i=1, 2, \dots, L} = \begin{cases} S & \text{if } i = 1 \text{ or } \theta_i > K \\ \text{flip}lr(S) & i = 2 \\ [S(1, \theta_i: \max(S)), S(1, 1: \theta_i - 1)] & i > 2 \text{ and } \theta_i \leq K \end{cases} \quad (4.19)$$

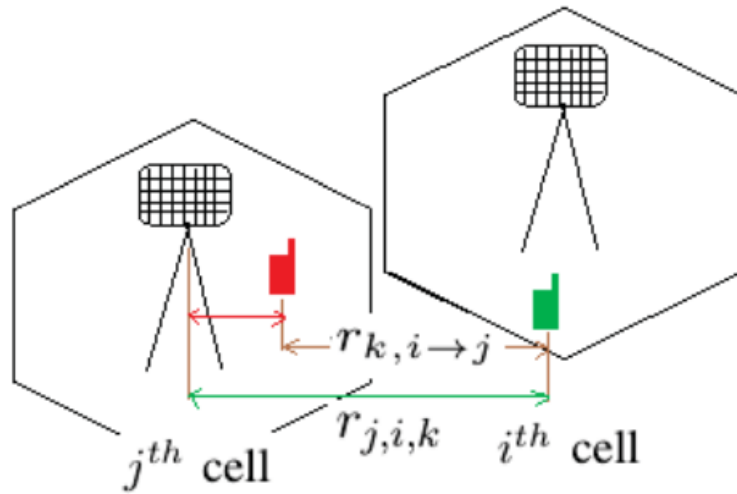


**Fig. 4.7:-**Distance between two users -of different cells- that employ the same pilot


Where  $\theta_i = 2i - 3$ , and  $\text{flip}(\text{vector})$  is the rotation of a vector by  $\pi$  (e.g.  $\text{flip}([1 \ 2 \ 3]) = [3 \ 2 \ 1]$ ). Notice that eqn. and during the process of constructing the matrix  $P$ , it is possible to find that two pilots are assigned to two users, which are close to each other in the matrix  $P$  (e.g. Fig.4.9, where we have considered  $d_{\text{step}} = 1$ ), leading in fact to generating severe contamination. Hence, to avoid this constraint, the proposed algorithm checks the following constraint:

For  $\{i = (1, 2, \dots, 7), k = 1, \dots, K\}$ , check if:

$$P(i, k) = \{P(i - d_{\text{step}}, k - d_{\text{step}}), P(i - d_{\text{step}}, k), P(i - d_{\text{step}}, k), P(i - d_{\text{step}}, k + d_{\text{step}}), P(i + d_{\text{step}}, k + d_{\text{step}}), P(i + d_{\text{step}}, k), P(i + d_{\text{step}}, k + d_{\text{step}})\} \quad (4.20)$$

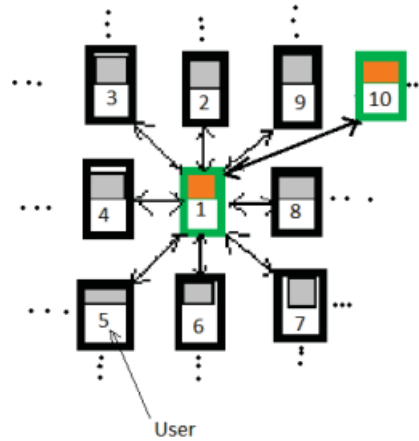


**Fig. 4.8:-** The user, which is indexed by one, is assigned with the pilot sequences  $\phi_1$ , where the proposed algorithm does not allow the reuse of the same pilots for the surrounded users i.e., 2,3...9, whereas  $\phi_1$  can be used for the user 10

Pilot sequences	$P(i, :) = [\phi^{[2]}, \phi^{[K]}, \dots, \phi^{[3]}]$
<i>LSF coefficients</i>	$\beta_i = [\beta_{i,i,1}, \beta_{i,i,K}, \dots, \beta_{i,i,3}]$
Users	

**Fig.4.9:-** Pilot Assignment based on the received P from the network hub

If Pilot Contamination mitigation by fractional pilot reuse with threshold optimisation in massive MIMO systems is satisfied once, then the pilot in  $P(i,k)$  is replaced by a new orthogonal pilot sequence. Once, the matrix P is constructed, the network hub sends the  $i$  th row of P to the  $i$  th BS (and so on for all BSs of the same cluster), then each BS assigns the received vector of pilots to its supported users where the  $k$ th user having the LSF coefficient  $\beta_{j,i,k}$  is assigned with the pilot of the  $k$ th position in the received pilot assignment vector and so on for the rest of users as depicted in Fig. 4.9.

The proposed algorithm is summarized in the Algorithm below. Notice that if the number of the considered cells is greater than seven, then the L cells are divided into clusters of seven cells and the same analysis presented above can be repeated for each cluster. Also, the complexity of this method is much better and

requires less time as compared to other methods to find the optimal pilot allocation for users in different cells.

#### 4.4.3.2 Algorithm for the Method based on LSFC

- 1: Input: System parameters  $d_{step}, K, L, S, \mu, \beta_{j,j,K} / \{j = 1, \dots, L : k = 1, 2, \dots, K\}$ .
- 2: Output: The matrix of pilot assignment  $P$ , the number of pilot requirement  $S$ .
- 3: Each BS constructs a vector of its corresponding  $LSF^{coefficients}$  classified in descendent order (10).
- 4: BSs send their corresponding vectors  $\beta_j$ , for  $j = 1, 2, \dots, L$ , to a network hub.
- 5: The network hub arranges the received vectors in a matrix of classification (11).
- 6: Based on (12) and (13), the network hub constructs the matrix of pilot assignment (i.e P).
- 7: For  $j = 1, \dots, L$ , the network hub sends the  $j^{th}$  row of P to the  $j^{th}$  BS.
- 8: BSs assign the received vectors to their supported users i.e  $\{\beta_{j,j,k} \leftarrow P(j, k)\}$  for  $\{j = 1, \dots, L : k = 1, 2, \dots, K\}$ .
- 9: end.

#### 4.4.3.3 LSFC Algorithm Outline and Summary

This Method is proposed for the purpose of pilot assignment which is mainly based on the user's large scale fading coefficients. Since the users' large scale fading coefficients depend on the distance between BSs and users, we have exploited this characteristic to classify users based on their LSF coefficients. Thereafter, pilots are assigned to users of different cells. Specifically, orthogonal pilots are assigned to users of different cells, which are close to each other. Accordingly, the problem of pilot contamination is largely reduced. The complexity of the algorithm is comparatively less and is faster for smaller  $d_{step}$ . If the  $d_{step}$  is  $> 4$ , then the algorithm might not be of the best use, because of the pilot overhead and thereby it loses its effectiveness.



## 4.5 Comparison of Method :

**Table 4.1 Comparison of the Two Methods of Interest**

<b>PARAMETER</b>	<b>SPRS +WGC-PD</b>	<b>LSFC</b>
Working of the method	All users are separated into two categories based on a parameter using SPRS method to get rid of the severe contamination. Then, in order to improve the decontamination of cell centred users, a weighted-graph-based method (WGC) is applied.	This technique assigns pilots to users of different cells based on their LSF coefficients. Specifically, the large-scale fading coefficients (LSFs) are exploited to show that the PC upon users depends on the distance between users that employ the same pilots.
Advantages of the method	This technique is proposed to mitigate PC for multi-cell massive MIMO systems and improve the QoS for the edge users	This technique aims to show that the PC upon users depends on the distance between the users that employ the same pilots.
Average uplink achievable rate(R) against N	The Average uplink achievable rate against the no. of antennas in BS is higher than that of SPRS and WGC methods individually.	The Average uplink achievable rate against the no. of antennas in BS is higher than that of WGC-PD and SPRS and both combined too.

<b>PARAMETER</b>	<b>SPRS+WGC-PD</b>	<b>LSFC</b>
SINR	SINR is better as compare to the other techniques.	It improves the SINR of the considered users substantially.
Time Complexity	Time Complexity: $O(M(K_e^2+K_c^2))$	Time Complexity: Low Complexity

# CHAPTER 5

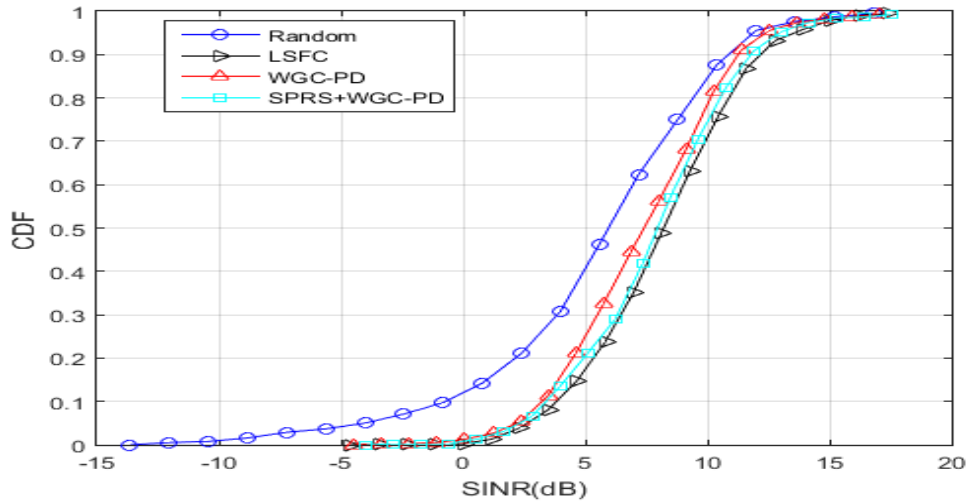
## Results and Discussions

### 5.1 Simulation Results

In this section, we evaluate the performance of the two methods of interest to mitigate PC in Massive MIMO through a set of Monte Carlo simulations. We consider a system of  $L$  hexagonal cells, where each cell is centered by a BS of  $M$  antennas, serving  $K$  single-antenna users. The parameters used in our simulations are given in Table 5.1. Herein, we compare the benefits of our proposed algorithms to both the Conventional Strategy, which is the random allocation procedure and the weighted graph coloring WGC scheme, which is proven to be one of the better methods to mitigate PC previously. Therefore, the 4 methods we have implemented to compare different parameters are the Conventional Strategy (Random Allocation), the LSFC strategy, the WGC method and finally the SPRS+WGC-PD method.

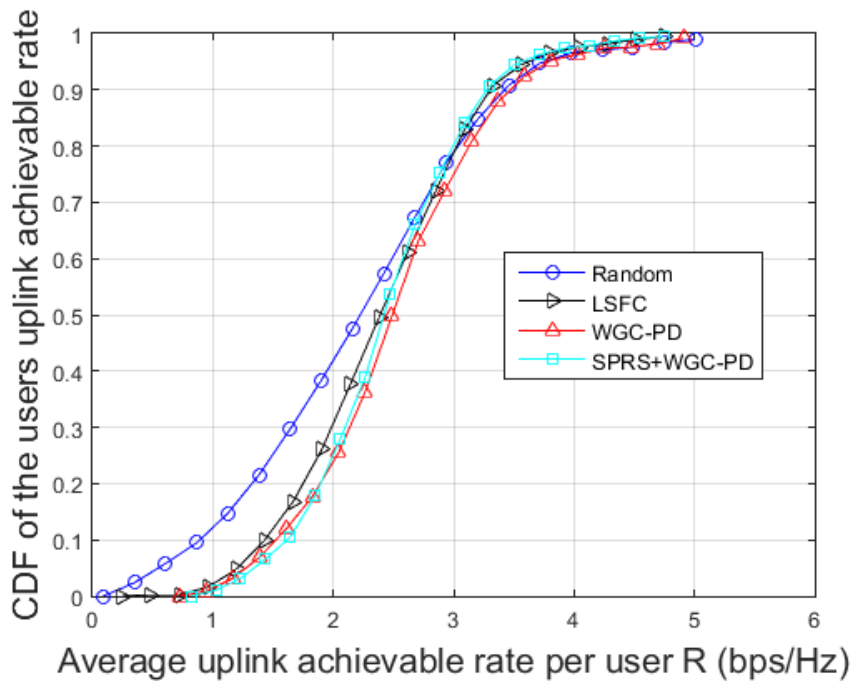
**Table 5.1 Parameters in simulation:**

Number of users in one cell $K$	10
Number of cells $J$	19
Number of pilot sequences $Q$	$K \leq Q \leq KJ$ 15 if fixed
Loss of spectral efficiency $\mu_0$	0.05
Antenna's number in a BS $N$	32~2048 128 if fixed
The threshold parameter $\theta$	$0.05 \leq \theta \leq 1$ 0.1 if fixed
Transmission power $\delta_p$	5~30 dB 15 if fixed
The shadowing fading $\sigma$	8 dB



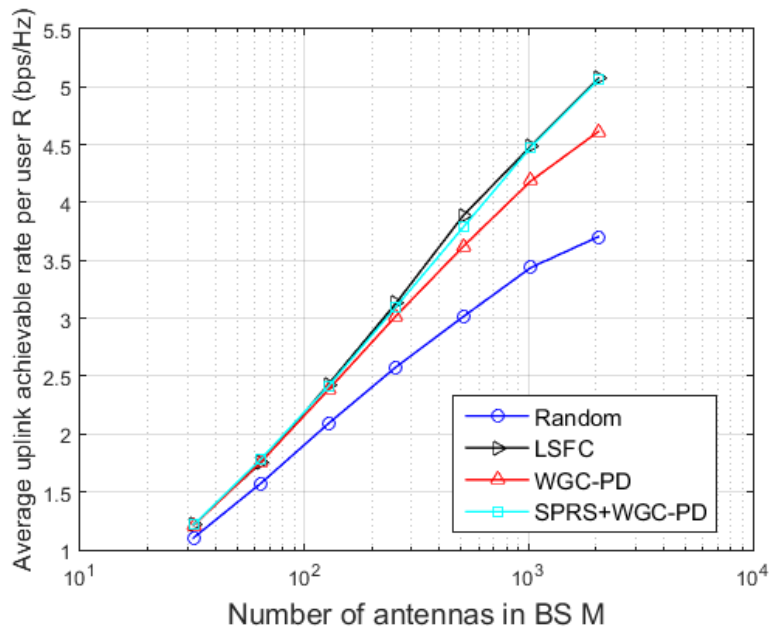
**Figure 5.1** CDF of uplink SINR for different schemes

Fig.5.1 shows the cumulative distribution function (CDF) of uplink SINR for different schemes considered. It is evident from the simulation result that the LSFC method, attains a fairly higher SINR for uplink users than both of SPRS+WGC-PD method and WGC-PD scheme respectively. The Random pilot scheme performs worst evidently. We know that higher the SINR, the better it is. Though the LSFC, WGC-PD, SPRS+WGC-PD have similar SINR, the LSFC stands out followed by the SPRS+WGC-PD method. In other words, with the same SINR value  $SINR_0$ , the order of the values of CDF is  $Random > WGC-PD > SPRS+WGC-PD > LSFC$ , which means that the LSFC scheme has the least users whose SINR are less than  $SINR_0$ . Therefore the probability that the users have higher SINR, while using LSFC scheme to allocate pilots is more than the other different schemes considered.



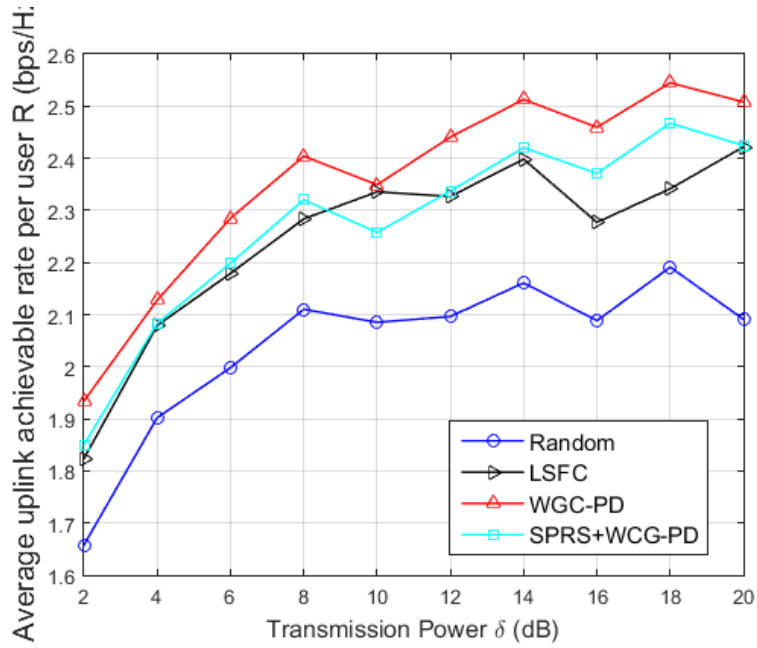
**Figure 5.2** CDF of uplink achievable rate R for different schemes

Fig.5.2 shows the relationship between CDF and rate R. It can be concluded that the LSFC scheme is superior to the other schemes initially, but the WGC scheme outperforms the other schemes gradually. And when R comes to about 5 bps/Hz, the CDF curves are all nearly reaching to 1. The Random allocation scheme again doesn't perform well when compared to the other schemes.



**Figure 5.3** Average uplink achievable rate  $R$  against Number of antennas  $M$  at the BS

Fig.5.3 shows the curves of rate  $R$  against  $M$ . It is obvious that with the increase of  $M$  (the number of antennas at the BS), the rates of these four schemes all rise. But evidently, from the simulation result the LSFC scheme's curve rises the fastest and achieves better rates when  $M$  is increased gradually. The next two schemes WGC-PD and SPR+WGC-PD also attain good rates as the  $M$  increases. Finally, the Random allocation scheme doesn't perform ideally and performs the worst in comparison.



**Figure 5.4** Average uplink achievable rate  $R$  against Transmission Power  $\rho$  (dB)

Fig.5.4 shows the curves of the rate  $R$  against the transmission power  $\rho$ , where the system parameters  $L = 19$ ,  $K = 10$ ,  $S = 25$ , and  $M = 128$  are considered. All the considered schemes can improve the rate  $R$  when  $\delta$  increases. At the same time, the LSFC and SPRS+WGC-PD work closely and perform similarly and the LSFC has a slightly better edge over the latter. Whereas the WGC method outperforms all the considered schemes as the transmission power is increased.

## CONCLUSIONS

In this project, we have studied , various methods that were proposed to mitigate the effects of pilot contamination in Massive MIMO. Most importantly, we have compared the two most promising methods that could reduce the severity of PC to a large extent in Massive MIMO systems. The two methods of interest are a novel decontamination method based on Soft Pilot Reuse clubbed with Weighted Graph Coloring and the Large-Scale Fading Coefficient Strategy. Simulation results showed that the LSFC strategy was able to mitigate PC up to a good extent and is a promising method to mitigate PC in Massive MIMO.

Massive MIMO has been recognized as a promising technology to meet the demand for higher data capacity for mobile networks. Although promising, each base station needs accurate estimation of the channel state information (CSI), either through feedback or channel reciprocity schemes in order to achieve the benefits of massive MIMO in practice. A popular scheme for estimating the wireless channel is through the transmission of pilot or training symbols. Pilot symbols are a predetermined fixed set of symbols which are transmitted over the wireless channel. The use of non-orthogonal pilot schemes, proposed for channel estimation in multi-cell TDD networks, is considered as a major source of pilot contamination in the literature due to the limitations of coherence time. So, in this project, we have investigated various methods to mitigate the effects of pilot contamination through our literature survey. The project was instantiated by introducing ourselves with what MIMO was, what the advantages of MIMO were, what Massive MIMO was as stated in Chapter 1. Then different terms and concepts related to Massive MIMO were investigated and studied. The importance of Channel Estimation and the use of pilots were extensively studied through various papers and text books and thus, finally the concept of pilot contamination was introduced. Many methods/schemes/algorithms were extensively investigated and studied to mitigate PC in Massive MIMO. After thorough literature survey, these were the methods/schemes that were studied to mitigate PC:

1. Smart Pilot Allocation [4]
2. Soft Pilot Reuse Scheme [6]
3. Weighted Graph Coloring Method [7]



4. Soft Pilot Reuse + Weighted Graph Coloring Method [10][11]
5. Strategy based on Large Scale Fading Coefficients [13]

Out of the various schemes studied as mentioned above, methods 4 and 5 looked promising in terms of complexity and severity of PC through simulation results and were studied in depth in order to provide an optimal solution to the problem of PC.

The two methods of interest, SPRS+WGC-PD and the LSFC Strategy are studied and compared as mentioned in Chapter 4. Initial parameters were defined and initialized. The algorithms of both the methods were implemented using Monte Carlo Simulations.

The performance of the above-mentioned methods was compared with the Conventional Strategy which is the Random Pilot Assignment, which doesn't take the PC severity into account and the Weighted Graph Coloring Scheme [4], which showed significant reduction of PC. Therefore the 4 methods considered for comparison are:

1. Random Pilot Assignment
2. LSFC strategy
3. Weighted Graph Coloring (WGC)
4. SPRS+WGC-PD

The 4 methods taken into account were compared based on few parameters like the SINR, uplink achievable rates  $R$ , achievable rates vs no of antennas to observe the performance of the methods when the no of antennas at the BS were increased and the uplink achievable rates when transmission power  $p$  is increased. The insights from the simulation results were as follows:

1. The LSFC strategy provided the best SINR values amongst the 4 methods compared, while the WGC method and the novel decontamination method had similar performance
2. The LSFC strategy was also the clear winner in the average uplink achievable rates  $R$  when compared to other methods

3. The Conventional Strategy which is the Random pilot assignment performed the worst in all cases.
4. When the number of antennas at the BS ( $M$ ) were increased, all the schemes had a rise in uplink achievable rates  $R$ , but the LSFC strategy and the SPRS+WGC-PD method showed substantial and promising increase in uplink rates.

Therefore, after thorough literature survey and simulation results, the LSFC Strategy and the novel decontamination method (SPRS+WGC) were able to mitigate PC up to a good extent, but the LSFC strategy could be a better scheme to implement as it is flexible, has better time complexity and provides better SINR and uplink achievable rates. Also, the pilot overhead drawback of SPRS+WGC is the main reason why the LSFC could be a better solution for this problem of PC.

## REFERENCES

- [1] T. L. Marzetta, "Noncooperative Cellular Wireless with Unlimited Numbers of Base Station Antennas", *IEEE Transactions on Wireless Communications*, vol. 9, no. 11, pp. 3590-3600, November 2010.
- [2] K. Zheng, Y. Wang, C. Lin, X. Shen, and J. Wang, "Graph-based interference coordination scheme in orthogonal frequency-division multiplexing access femtocell networks," *IET Commun.*, vol. 5, no. 17, pp. 2533–2541, Nov. 2011.
- [3] X. Zhu, L. Dai and Z. Wang, "Graph Coloring Based Pilot Allocation to Mitigate Pilot Contamination for Multi-Cell Massive MIMO Systems," in *IEEE Communications Letters*, vol. 19, no. 10, pp. 1842-1845, Oct. 2015.
- [4] X. Zhu, Z. Wang, L. Dai and C. Qian, "Smart Pilot Assignment for Massive MIMO," in *IEEE Communications Letters*, vol. 19, no. 9, pp. 1644-1647, Sept. 2015.
- [5] O. Elijah, C. Y. Leow, T. A. Rahman, S. Nunoo and S. Z. Iliya, "A Comprehensive Survey of Pilot Contamination in Massive MIMO-5G System", *IEEE Communications Surveys & Tutorials*, vol. 18, no. 2, pp. 905-923, Second quarter 2016.
- [6] X. Zhu et al., "Soft Pilot Reuse and Multicell Block Diagonalization Precoding for Massive MIMO Systems," in *IEEE Transactions on Vehicular Technology*, vol. 65, no. 5, pp. 3285-3298, May 2016.
- [7] X. Zhu, L. Dai, Z. Wang and X. Wang, "Weighted-Graph-Coloring-Based Pilot Decontamination for Multicell Massive MIMO Systems," in *IEEE Transactions on Vehicular Technology*, vol. 66, no. 3, pp. 2829-2834, March 2017.
- [8] Abdelhamid Riadi, Mohamed Boulouird and Moha M'Rabet Hassani, "An Overview of Massive-MIMO in 5G Wireless Communications", *Colloque International TELECOM 2017 & 10èmes JFMMA EMI -Rabat*, Mai 10-12, 2017.
- [9] M. Boulouird, A. Riadi and M. M. Hassani, "Pilot contamination in multi-cell massive-MIMO systems in 5G wireless communications", *2017 International Conference on Electrical and Information Technologies (ICEIT)*, pp. 1-4, 2017.
- [10] Yuan, W., Yang, X., & Xu, R. (2018). "A novel pilot decontamination scheme for uplink massive MIMO systems". *Procedia Computer Science*, 131, 72–79.

- [11] W. Chang, H. Chan and Y. Hua, "Weighted Graph Coloring Based Softer Pilot Reuse for TDD Massive MIMO Systems," in *IEEE Transactions on Vehicular Technology*, vol. 67, no. 7, pp. 6272-6285, July 2018.
- [12] A. Belhabib, M. Boulouird and M. M. Hassani, "The Impact of Using Additional Pilots on the Performance of Massive MIMO Systems," 2019 International Conference on Signal, Control and Communication (SCC), 2019, pp. 87-92.
- [13] A. BELHABIB, M. BOULOUIRD and M. M. HASSANI, "New Strategy based on Large Scale Fading Coefficients to Mitigate the Pilot Contamination Problem in Massive MIMO Systems," *2020 IEEE 2nd International Conference on Electronics, Control, Optimization and Computer Science (ICECOCS)*, 2020, pp. 1-6.

